

AFRL-IF-RS-TR-1998-169

Final Technical Report

August 1998



ENHANCED TIME DOMAIN INTERFERENCE SUPPRESSION TECHNIQUES

Rensselaer Polytechnic Institute

Gary J. Saulnier

APPROVED FOR PUBLIC RELEASE; DISTRIBUTION UNLIMITED.

19981015 098

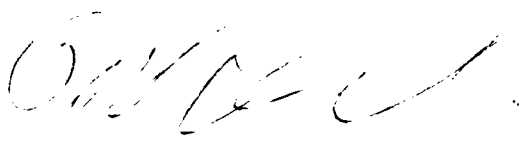
**AIR FORCE RESEARCH LABORATORY
INFORMATION DIRECTORATE
ROME RESEARCH SITE
ROME, NEW YORK**

DTIC QUALITY INSPECTED 4

This report has been reviewed by the Air Force Research Laboratory, Information Directorate, Public Affairs Office (IFOIPA) and is releasable to the National Technical Information Service (NTIS). At NTIS it will be releasable to the general public, including foreign nations.

AFRL-IF-RS-TR-1998-169 has been reviewed and is approved for publication.

APPROVED: 
MICHAEL J. MEDLEY
Project Engineer

FOR THE DIRECTOR: 
WARREN H. DEBANY, JR., Technical Advisor
Information Grid Division
Information Directorate

If your address has changed or if you wish to be removed from the Air Force Research Laboratory Rome Research Site mailing list, or if the addressee is no longer employed by your organization, please notify AFRL/IFGC, 525 Brooks Road, Rome, NY 13441-4505. This will assist us in maintaining a current mailing list.

Do not return copies of this report unless contractual obligations or notices on a specific document require that it be returned.

REPORT DOCUMENTATION PAGE			Form Approved OMB No. 0704-0188	
Public reporting burden for this collection of information is estimated to average 1 hour per response, including the time for reviewing instructions, searching existing data sources, gathering and maintaining the data needed, and completing and reviewing the collection of information. Send comments regarding this burden estimate or any other aspect of this collection of information, including suggestions for reducing this burden, to Washington Headquarters Services, Directorate for Information Operations and Reports, 1215 Jefferson Davis Highway, Suite 1204, Arlington, VA 22202-4302, and to the Office of Management and Budget, Paperwork Reduction Project (0704-0188), Washington, DC 20503.				
1. AGENCY USE ONLY (Leave blank)	2. REPORT DATE August 1998	3. REPORT TYPE AND DATES COVERED Final Jun 97 - Sep 97		
4. TITLE AND SUBTITLE ENHANCED TIME DOMAIN INTERFERENCE SUPPRESSION TECHNIQUES		5. FUNDING NUMBERS C - F30602-97-1-0206 PE - 61102F PR - 2304 TA - C7 WU - 05		
6. AUTHOR(S) Gary J. Saulnier				
7. PERFORMING ORGANIZATION NAME(S) AND ADDRESS(ES) Rensselaer Polytechnic Institute 110 Eighth Street Troy, NY 12180-3590		8. PERFORMING ORGANIZATION REPORT NUMBER N/A		
9. SPONSORING/MONITORING AGENCY NAME(S) AND ADDRESS(ES) AFRL/IFGC 525 Brooks Road Rome, NY 13441-4505		10. SPONSORING/MONITORING AGENCY REPORT NUMBER AFRL-IF-RS-TR-1998-169		
11. SUPPLEMENTARY NOTES AFRL Project Engineer: Michael J. Medley/IFGC/(315) 330-4830				
12a. DISTRIBUTION AVAILABILITY STATEMENT Approved for public release; distribution unlimited.		12b. DISTRIBUTION CODE		
13. ABSTRACT (Maximum 200 words) Many methods have been proposed for suppressing interference in a direct sequence spread spectrum signal and a number of these utilize adaptive transversal suppression filters to remove a large portion of the interference prior to despreading. This report investigates the performance of predictive and two-sided adaptive filtering systems and presents a method to improve the performance of the predictive filter by compensating for the distortion introduced into the desired direct sequence signal during the adaptive filtering process. It is shown that the predictive filter acts as a pre-whitener and the two-sided filter acts as a power inverter. Additionally, the two-sided adaptive filter automatically performs the same function as the compensated predictive filter. The performance of the adaptive systems is also studied when there is multipath propagation and it is shown that the presence of multipath allows the filters to partially suppress the desired direct sequence signal, resulting in performance loss. A combination of simulation and analysis was used to perform this study. Simulations were performed using the Signal Processing Work System (SPW) from Alta Group of Cadence Design Systems, Inc.				
14. SUBJECT TERMS Adaptive Filtering, Multipath Propagation, Interference Suppression, Jamming		15. NUMBER OF PAGES 56		
		16. PRICE CODE		
17. SECURITY CLASSIFICATION OF REPORT UNCLASSIFIED	18. SECURITY CLASSIFICATION OF THIS PAGE UNCLASSIFIED	19. SECURITY CLASSIFICATION OF ABSTRACT UNCLASSIFIED	20. LIMITATION OF ABSTRACT UL	

Contents

1	Introduction	1
1.1	Program Objective	1
1.2	Report Organization	1
2	Time Domain Adaptive Filter Suppressors	3
2.1	Predictive Pre-Whitening Filter	4
2.2	Two-Sided Adaptive Filter	5
3	Filter Responses	7
3.1	Analytical Wiener Responses	7
3.1.1	Predictive Filter	7
3.1.2	Two-Sided Filter	9
3.2	Comparison of Frequency Responses	10
4	Filter Compensation	15
5	SPW Simulation	18
5.1	Test Signal Generation	18
5.2	Adaptive Filters	18
5.3	Test Systems	21

6	Performance Results	23
6.1	AWGN and Interference	23
6.2	Multipath Channel	34
7	Summary and Conclusions	40
7.1	Future Work	41
7	Bibliography	42

List of Figures

2.1	Predictive Transversal Filter	4
2.2	Direct Sequence System using a Pre-whitening Anti-jam Receiver	5
2.3	Two-Sided Transversal Filter	6
3.1	Comparison of filter frequency responses, order = 10, JSR = 20 dB.	11
3.2	Output spectrum for the two-sided filter.	12
3.3	Output spectrum for the predictive filter.	13
3.4	Comparison of frequency responses for order = 5, JSR = 30 dB.	13
3.5	Comparison of frequency responses for order = 10, JSR = 30 dB.	14
3.6	Comparison of frequency responses for order = 20, JSR = 30 dB.	14
4.1	Tapped delay line channel model.	15
4.2	One form of the RAKE receiver.	16
4.3	Compensated adaptive filter receiver.	17
5.1	Signal Generation in SPW	19
5.2	Predictive adaptive filter suppressor.	19
5.3	Two-sided adaptive filter suppressor.	20
5.4	Compensated predictive adaptive filter suppressor.	20
5.5	Compensated two-sided adaptive filter suppressor.	21

6.1	BER vs. E_b/N_o for a single tone jammer with frequency = 0.234 and JSR = 20 dB. Filter order = 10.	24
6.2	BER vs. E_b/N_o for a narrowband Gaussian jammer with frequency 0.234 and bandwidth 0.1. Filter order = 20.	26
6.3	BER vs. E_b/N_o for a narrowband Gaussian jammer with frequency 0.234 and bandwidth 0.1. Filter order = 10.	27
6.4	BER vs. filter order for a narrowband Gaussian jammer with frequency 0.234 and bandwidth 0.1. E_b/N_o = 6 dB.	28
6.5	BER vs. jammer bandwidth for a narrowband Gaussian jammer with frequency 0.234 and JSR = 20 dB. E_b/N_o = 10 dB.	29
6.6	BER vs. E_b/N_o for a narrowband Gaussian jammer with frequency 0.234, bandwidth = 0.1 and JSR = 20 dB. Included is the result when the residual jammer energy is removed from the output.	31
6.7	Overlay of the impulse responses of the compensated predictive filter (dashed) and the two-sided filter (solid). E_b/N_o =10 dB, JSR = 30 dB, frequency = 0.234 and bandwidth = 0.1.	32
6.8	Overlay of the frequency responses of the compensated predictive filter (dashed) and the two-sided filter (solid). E_b/N_o =10 dB, JSR = 30 dB, frequency = 0.234 and bandwidth = 0.1.	33
6.9	BER performance of the predictive adaptive suppressor with a two-ray multipath channel and no interference.	35
6.10	BER performance of the two-sided adaptive suppressor with a two-ray multipath channel and no interference.	36
6.11	BER performance of the predictive adaptive suppressor with a two-ray multipath channel and interference. Interference frequency = 0.234, bandwidth = 0.1 and JSR = 20 dB.	37
6.12	BER performance of the two-sided adaptive suppressor with a two-ray multipath channel and interference. Interference frequency = 0.234, bandwidth = 0.1 and JSR = 20 dB.	38
6.13	BER performance of the predictive and two-sided adaptive suppressors with a two-ray multipath channel and interference. Interference frequency = 0.1176, bandwidth = 0.1 and JSR = 20 dB.	39

Chapter 1

Introduction

1.1 Program Objective

Many methods have been proposed for suppressing interference in a direct sequence spread spectrum signal and a number of these utilize adaptive transversal suppression filters to remove a large portion of the interference prior to despreading. The objective of this effort was to study the performance of these adaptive filtering systems and to improve their performance by compensating for the distortion introduced into the desired direct sequence signal during the adaptive filtering process. The overall goal was to produce a low-complexity adaptive suppressor that can rapidly adapt to changing interference environments. A second objective was to investigate the effect of multipath propagation on the the performance of these interference mitigation techniques and to consider ways to combine the energy in the multiple received paths. A combination of simulation and analysis was used to perform this study. Simulations were performed using the Signal Processing WorkSystem (SPW) from AltaGroup of Cadence Design Systems, Inc.

1.2 Report Organization

The next chapter provides some background on the predictive and two-sided adaptive filters which are the primary focus of this investigation. In Chapter 3 analytical expressions are obtained for the tap weights for both types of filters and the resulting frequency responses are compared. Chapter 4 introduces the idea of using a compensating filter after the adaptive suppressor in order to mitigate the distortion introduced during the suppression process while Chapter 5 describes the systems that were built in SPW to investigate the performance of the techniques. Chapter 6 presents performance results for the various systems, mostly in the form of bit-error-rate (BER) values obtained through Monte Carlo simulation. Finally,

Chapter 7 summarizes the work performed during the effort and the major results that were obtained and presents some topics for further investigation.

Chapter 2

Time Domain Adaptive Filter Suppressors

Many methods have been proposed for suppressing interference in a direct sequence spread spectrum signal [1]. A number of these utilize transversal suppression filters to remove a large portion of the interference prior to despreading, including [2, 3, 4, 5, 6, 7]. In [2], pre-whitening transversal filters are designed according to Wiener and maximum entropy methods. Here, past samples of the received signal are used to generate an estimate of the current value of the interference. This estimate is then subtracted from the signal to form an estimate of the direct sequence signal. In [3], a two sided transversal filter is introduced that uses both the past and future values of the incoming signal to predict the current sample and, in the process, suppress narrowband interference. Two adaptive suppression techniques are introduced in [4], an FFT spectral analysis technique and a parametric linear prediction method. In [5] an adaptive receiver is presented that uses bit decisions to create an estimate of the transmitted signal, which is then subtracted from the received signal to form an estimate of the interference. The algorithm whitens this estimate of the interference and then uses the same filter coefficients to filter the received signal.

Other time-domain adaptive filter-based techniques have been proposed which work in a decision-directed mode to produce a minimum mean square error (MMSE) estimate of the transmitted data sequence. One of these techniques is the *adaptive correlator* receiver described in [8]. These techniques provide improved bit-error rate (BER) performance but require the use of a training sequence. Additionally, the adaptive algorithm can be iterated only once per *symbol* rather than once per *chip*, resulting in a large increase in convergence time, particularly for large processing gains, and the associated reduction in the ability to track rapidly changing interference environments.

This effort will focus on improving the performance of transversal filter suppressors which operate *blind*, i.e. without a training sequence, by compensating for the distortion

introduced into the desired direct sequence signal during the adaptive suppression process. As a result, the main focus is on the predictive and two-sided adaptive transversal filter structures. The goal is to produce a low-complexity adaptive suppressor that can rapidly adapt to changing interference environments. A second objective is to investigate ways of coupling this interference mitigation technique with a system for combining the energy in multiple received paths.

2.1 Predictive Pre-Whitening Filter

A simple predictive adaptive filter interference suppression structure is shown in Figure 2.1 [2, 4, 7, 5, 9]. In this system, the input signal $x[k]$ consists of a direct sequence spread spectrum

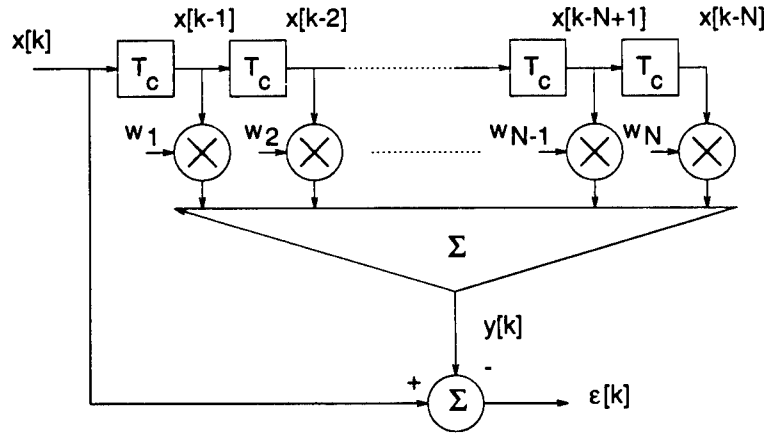


Figure 2.1: Predictive Transversal Filter

signal, additive white Gaussian noise (AWGN) and interference. This composite signal is fed into a tapped delay structure having a tap spacing equal to the chip duration, T_c . Delayed input samples, $x[k-1]$, $x[k-2]$, ..., $x[k-N]$ are multiplied by a set of tap weights, w_1 , w_2 , ..., w_N , and the products are summed to form the signal $y[k]$. This output is then subtracted from the input signal to form an error signal, $\epsilon[k]$.

The tap weights are determined using an adaptive algorithm which works to minimize the error signal, $\epsilon[k]$. This adaptive process forces $y[k]$ to become an estimate of the current sample of the input signal, $x[k]$, that is based on *past samples* of the input signal, $x[k-1]$, $x[k-2]$, ..., $x[k-N]$. For the direct sequence signal and the AWGN, the fact that samples of these signals are poorly correlated makes the system unable to form an accurate estimate of the most recent sample based on the past samples. Consequently, $y[k]$ will not contain an estimate of the direct sequence signal and the AWGN. However, if the interference is narrowband, its samples will be highly correlated and $y[k]$ will be an accurate estimate of

the interference. The error signal, then, will become an estimate of the uncorrelated portion of the input, i.e. the direct sequence signal and AWGN.

Due to the behavior described above, the structure shown in Figure 2.1 is often called a *correlation canceler* or a *pre-whitening filter*. Since a white signal has an impulse function for its autocorrelation function, i.e. it is correlated only with zero shifts of itself, the two descriptions are identical. An anti-jam direct sequence receiver can be made using the adaptive suppressor by feeding the received signal first through the pre-whitening filter and then into a conventional correlation receiver as shown in Figure 2.2.

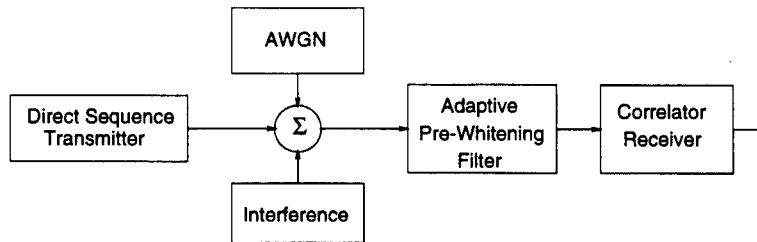


Figure 2.2: Direct Sequence System using a Pre-whitening Anti-jam Receiver

Many algorithms can be used to determine the tap weights for the adaptive suppressor. The two most common techniques are the Least-Mean Square (LMS) and Recursive Least Square (RLS) algorithms. Both these algorithms are *iterative*, meaning that they do not require information about the statistics of the incoming signal but, rather, adapt on a step-by-step basis to converge to the optimal (in the mean-square sense) tap weights. In the direct sequence receiver application, an iteration occurs each time a new sample is input into the delay line, meaning that the system adapts once per chip of the signal.

2.2 Two-Sided Adaptive Filter

There are several variations of this structure that can be used for suppressing interference. The most notable variation is the *two-sided* transversal filter, shown in Figure 2.3, in which an estimate of the current input sample is formed using both past and future samples of the signal. Direct sequence receivers using the two-sided structure to suppress narrowband interference have been shown to provide BER performance than receivers using the predictive filter structure [3]. The two-sided structure has the advantage that it creates a *linear phase* response, meaning that it does not introduce any group delay distortion into the signal. Additionally, the structure does not behave as a pre-whitening filter but, rather, operates more like a *power inverter*. In this case, the output spectrum resembles the inverse of the input spectrum where, for example, a portion of the input spectrum that is at +20 dB is

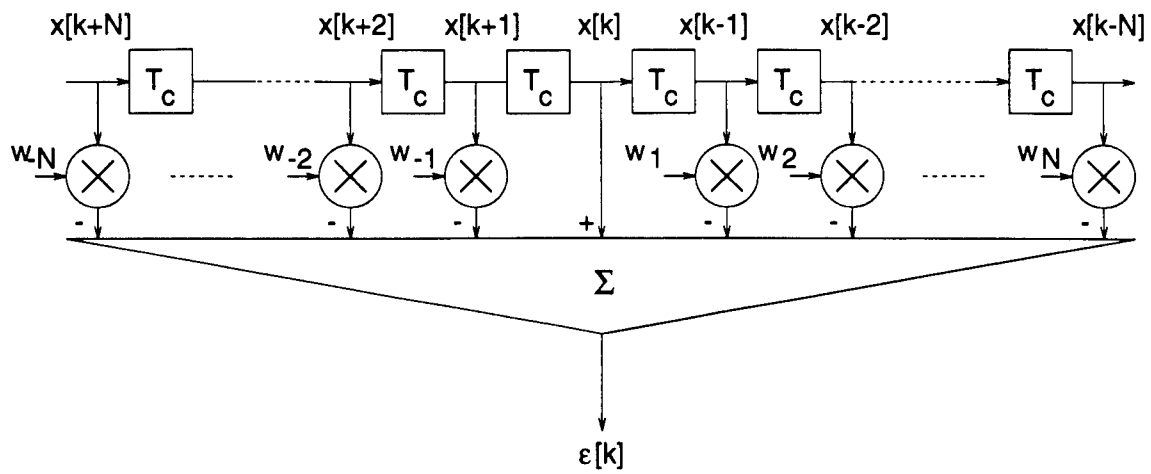


Figure 2.3: Two-Sided Transversal Filter

suppressed to -20 dB in the output. This property of the two-sided filter will be illustrated later.

Chapter 3

Filter Responses

In this chapter, we derive the Wiener response for both the predictive and two-sided transversal filter responses and use the results to illustrate and compare the behavior of the two filter types.

3.1 Analytical Wiener Responses

3.1.1 Predictive Filter

The input to the adaptive filter is given by $x[k]$ and the tap weights are given by $w_i[k]$. To simplify the derivation, vector notation will be used to represent these quantities. For a filter with N taps, the vector of samples in the delay line is given by

$$\mathbf{x}[k] = \begin{bmatrix} x[k-1] \\ x[k-2] \\ \vdots \\ x[k-N] \end{bmatrix}. \quad (3.1)$$

Since we will be deriving the Wiener response, there will not be a time dependence on the tap weights. The tap weight vector, then, is represented by

$$\mathbf{w} = \begin{bmatrix} w_1 \\ w_2 \\ \vdots \\ w_N \end{bmatrix}. \quad (3.2)$$

With this notation, the sum of the tap weights times the delayed input samples can be represented by

$$y[k] = \mathbf{w}^T \mathbf{x}[k] \quad (3.3)$$

and the corresponding error signal is

$$\begin{aligned} \varepsilon[k] &= x[k] - y[k] \\ &= x[k] - \mathbf{w}^T \mathbf{x}[k]. \end{aligned} \quad (3.4)$$

To determine the weight vector which produces the minimum mean-square error (MMSE), first square $\varepsilon[k]$ as given by (3.4) to get

$$\varepsilon^2[k] = x^2[k] - 2x[k]\mathbf{w}^T \mathbf{x}[k] + \mathbf{w}^T \mathbf{x}[k]\mathbf{x}^T[k]\mathbf{w}. \quad (3.5)$$

Now, evaluate the expected value of $\varepsilon^2[k]$,

$$E\{\varepsilon^2[k]\} = E\{x^2[k]\} - 2E\{\mathbf{w}^T x[k]\mathbf{x}[k]\} + E\{\mathbf{w}^T \mathbf{x}[k]\mathbf{x}^T[k]\mathbf{w}\}. \quad (3.6)$$

Since \mathbf{w} is a constant, it can be passed through the expectation operator, yielding

$$E\{\varepsilon^2[k]\} = E\{x^2[k]\} - 2\mathbf{w}^T E\{x[k]\mathbf{x}[k]\} + \mathbf{w}^T E\{\mathbf{x}[k]\mathbf{x}^T[k]\}\mathbf{w}. \quad (3.7)$$

To simplify (3.7), define the autocorrelation matrix of the input signal as

$$\begin{aligned} \mathbf{R} &= E\{\mathbf{x}[k]\mathbf{x}^T[k]\} \\ &= E\left\{\begin{bmatrix} x[k-1]x[k-1] & x[k-1]x[k-2] & \cdots & x[k-1]x[k-N] \\ x[k-2]x[k-1] & x[k-2]x[k-2] & \cdots & x[k-2]x[k-N] \\ x[k-3]x[k-1] & x[k-3]x[k-2] & \cdots & x[k-3]x[k-N] \\ \vdots & \vdots & \ddots & \vdots \\ x[k-N]x[k-1] & x[k-N]x[k-2] & \cdots & x[k-N]x[k-N] \end{bmatrix}\right\}. \end{aligned} \quad (3.8)$$

For a stationary input signal, $E\{x[k-m]x[k-n]\} = R[n-m]$, where $R[\alpha]$ denotes the autocorrelation function of the input signal. If the signal is also real, $R[\alpha]$ also has even symmetry and (3.8) can be rewritten as

$$\mathbf{R} = \begin{bmatrix} R[0] & R[1] & \cdots & R[N-1] \\ R[1] & R[0] & \cdots & R[N-2] \\ R[2] & R[1] & \cdots & R[N-3] \\ \vdots & \vdots & \ddots & \vdots \\ R[N-1] & R[N-2] & \cdots & R[0] \end{bmatrix}. \quad (3.9)$$

In the same way, the cross-correlation vector between $x[k]$ and the input vector

$$\begin{aligned} \mathbf{P} &= E\{x[k]\mathbf{x}[k]\} \\ &= E\left\{\begin{bmatrix} x[k]x[k-1] \\ x[k]x[k-2] \\ \vdots \\ x[k]x[k-N] \end{bmatrix}\right\} = \begin{bmatrix} R[1] \\ R[2] \\ \vdots \\ R[N] \end{bmatrix}. \end{aligned} \quad (3.10)$$

Using these new variables, (3.7) can be rewritten as

$$E \{ \varepsilon^2[k] \} = E \{ x^2[k] \} - 2\mathbf{w}^T \mathbf{P} + \mathbf{w}^T \mathbf{R} \mathbf{w}. \quad (3.11)$$

To determine the optimal weight vector, take the partial derivative of (3.11) with respect to \mathbf{w}

$$\frac{\partial E \{ \varepsilon^2[k] \}}{\partial \mathbf{w}} = -2\mathbf{P} + 2\mathbf{R} \mathbf{w} \quad (3.12)$$

and set the result equal to zero yielding,

$$\mathbf{R} \mathbf{w} = \mathbf{P}. \quad (3.13)$$

Rearranging (3.13) produces the Wiener-Hopf equation

$$\mathbf{w} = \mathbf{R}^{-1} \mathbf{P}. \quad (3.14)$$

3.1.2 Two-Sided Filter

For the two-sided filter, the tap weights are symmetrical around the center tap, e.g. $w_1 = w_{-1}$, $w_2 = w_{-2}$, etc.. Consequently, we will derive an expression for one side of the weights, the same weight vector as given by (3.2). To start, express the contents of the delay line by two separate vectors

$$\mathbf{x}_n[k] = \begin{bmatrix} x[k-1] \\ x[k-2] \\ \vdots \\ x[k-N] \end{bmatrix} \quad (3.15)$$

and

$$\mathbf{x}_p[k] = \begin{bmatrix} x[k+1] \\ x[k+2] \\ \vdots \\ x[k+N] \end{bmatrix} \quad (3.16)$$

The total contents of the delay line in Figure 2.3 are the samples in $\mathbf{x}_n[k]$, $\mathbf{x}_p[k]$ along with $x[k]$. The error signal, $\varepsilon[k]$, is given by

$$\begin{aligned} \varepsilon[k] &= x[k] - \mathbf{w}^T \mathbf{x}_p[k] - \mathbf{w}^T \mathbf{x}_n[k] \\ &= x[k] - \mathbf{w}^T (\mathbf{x}_p[k] + \mathbf{x}_n[k]). \end{aligned} \quad (3.17)$$

As with the predictive case, we must find the weight vector which produces the minimum mean-square error. Start by finding the square error

$$\varepsilon^2[k] = x^2[k] - 2x[k]\mathbf{w}^T (\mathbf{x}_p[k] + \mathbf{x}_n[k]) + \mathbf{w}^T (\mathbf{x}_p[k] + \mathbf{x}_n[k])(\mathbf{x}_p[k] + \mathbf{x}_n[k])^T \mathbf{w} \quad (3.18)$$

and then taking the expectation to produce

$$E \{ \varepsilon^2[k] \} = E \{ x^2[k] \} - 2\mathbf{w}^T E \{ x[k](\mathbf{x}_p[k] + \mathbf{x}_n[k]) \} + \mathbf{w}^T E \{ (\mathbf{x}_p[k] + \mathbf{x}_n[k])(\mathbf{x}_p[k] + \mathbf{x}_n[k])^T \} \mathbf{w}. \quad (3.19)$$

If it is assumed that the input signal is stationary,

$$E \{ x[k](\mathbf{x}_p[k] + \mathbf{x}_n[k]) \} = 2\mathbf{P} \quad (3.20)$$

where \mathbf{P} is defined in (3.10). Now consider the expectation in the third term on the right of (3.19). Expanding,

$$\begin{aligned} & E \{ (\mathbf{x}_p[k] + \mathbf{x}_n[k])(\mathbf{x}_p[k] + \mathbf{x}_n[k])^T \} \\ &= E \{ \mathbf{x}_p[k]\mathbf{x}_p^T[k] + \mathbf{x}_n[k]\mathbf{x}_p^T[k] + \mathbf{x}_p[k]\mathbf{x}_n^T[k] + \mathbf{x}_n[k]\mathbf{x}_n^T[k] \} \end{aligned} \quad (3.21)$$

Again, for a real, stationary input signal

$$E \{ \mathbf{x}_p[k]\mathbf{x}_p^T[k] \} = E \{ \mathbf{x}_n[k]\mathbf{x}_n^T[k] \} = \mathbf{R}, \quad (3.22)$$

where \mathbf{R} is defined in (3.9). Also,

$$E \{ \mathbf{x}_n[k]\mathbf{x}_p^T[k] \} = \begin{bmatrix} R[2] & R[3] & \cdots & R[N+1] \\ R[3] & R[4] & \cdots & R[N+2] \\ R[4] & R[5] & \cdots & R[N+3] \\ \vdots & \vdots & \vdots & \vdots \\ R[N+1] & R[N+2] & \cdots & R[N+N] \end{bmatrix} \triangleq \mathbf{G}, \quad (3.23)$$

where \mathbf{G} has the form of Hankel matrix. Using this notation, the mean-square error can be expressed as

$$E \{ \varepsilon^2[k] \} = E \{ x^2[k] \} - 4\mathbf{w}^T \mathbf{P} + 2\mathbf{w}^T \mathbf{R} \mathbf{w} + 2\mathbf{w}^T \mathbf{G} \mathbf{w}. \quad (3.24)$$

Taking the partial derivative with respect to \mathbf{w} , setting the result to zero and solving for \mathbf{w} yields an expression for the MMSE weight vector,

$$\mathbf{w} = [\mathbf{R} + \mathbf{G}]^{-1} \mathbf{P}. \quad (3.25)$$

3.2 Comparison of Frequency Responses

The expressions for the tap weights in both the predictive and two-sided filters were coded into **Matlab**. The SPW system of Figure 5.1 was used to generate a segment of the composite direct sequence spread spectrum (DSSS) plus AWGN plus jammer signal and the SPW Signal Calculator was used to produce the one-sided autocorrelation sequence, i.e.

$R[0], R[1], R[2], \dots$, for that signal. This autocorrelation sequence was used as the input to the **Matlab** and used to calculate the tap weights for both the predictive and two-sided filters. These weights are then used to generate the impulse responses for the filters and, subsequently, their frequency responses through the use of a Fast Fourier Transform (FFT).

Figure 3.1 compares the frequency response of the filters with a narrowband Gaussian jammer having a normalized center frequency of 0.234, normalized bandwidth of 0.1, Jammer to Signal Power Ratio (JSR) of 20 dB and energy per bit to one-sided noise power spectral density ratio (E_b/N_0) of 10 dB. The order of the filters is 10, meaning that the predictive filter has 10 variable tap weights and the two-sided filter has a total of 20 variable taps. Normalization is with respect to the chip rate. The figure also shows an estimate of

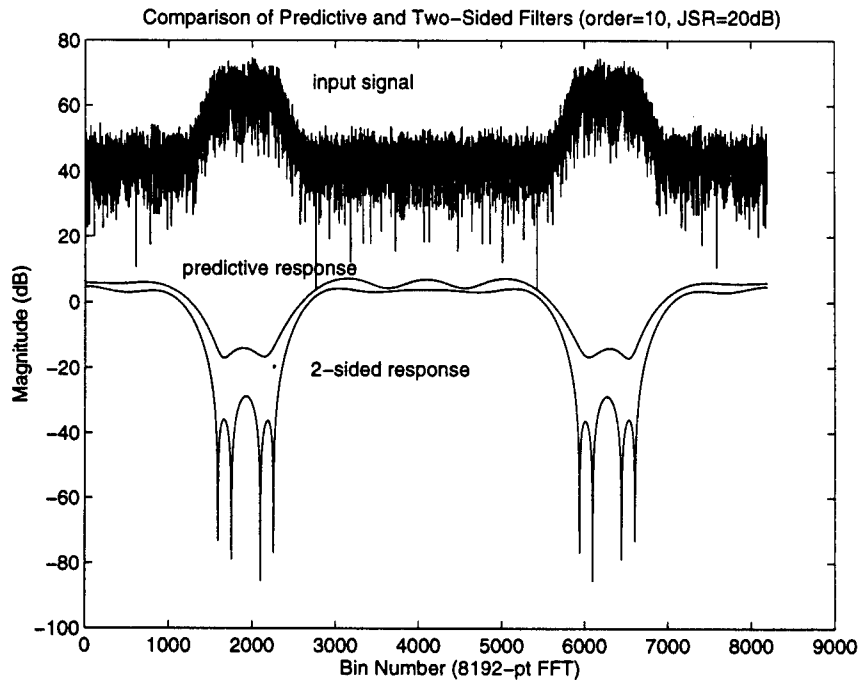


Figure 3.1: Comparison of filter frequency responses, order = 10, JSR = 20 dB.

the power spectrum of the input signal, obtained by plotting the magnitude squared of a FFT of a segment of the signal itself.

The first thing to note in Figure 3.1 is that the use of a sampling rate that is equal to the chip rate results in the aliasing of the jammer, meaning that the jammer produced by passing white Gaussian noise through a filter with a bandwidth of 0.1 times the chip rate actually affects 20% of the frequency band, as opposed to 10%. With respect to the frequency responses of the predictive and two-sided filters, it is clear that the predictive filter tends to act as a pre-whitener, since the response approximates the mirror image of the signal spectrum. Passing the signal through this frequency response does result in a

nearly white spectrum. To the contrary, the two-sided filter produces a notch at the jammer frequencies that is nearly twice as deep as is needed to whiten the input signal. As a result, the effect of passing the input signal through this filter will be to produce an output signal whose spectrum is nearly the mirror image of the input signal spectrum. Figures 3.2 and 3.3 show the output spectra for the two-sided and predictive filters, respectively.

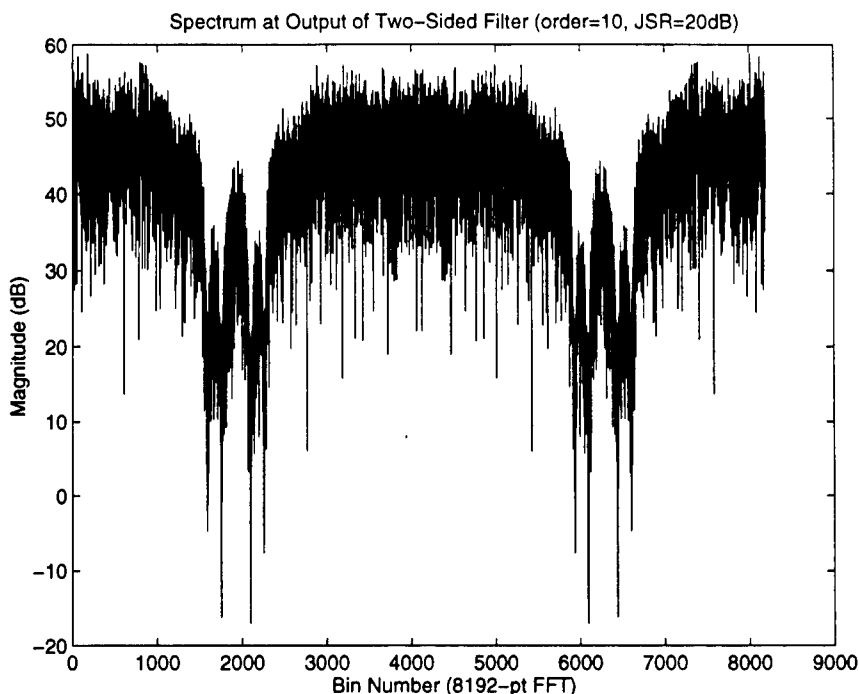


Figure 3.2: Output spectrum for the two-sided filter.

Quality of the response is clearly a function of the order of the filter. A higher order filter is better able to suppress the interference while less distortion in other parts of the spectrum. Figures 3.4, 3.5, and 3.6 show the filter responses when the JSR is 30 dB and the filter order is 5, 10 and 20, respectively. Note how the notch in the frequency responses become more ideal as the filter order increases but the depth of these notches does not vary with filter order. Note that the filter responses become flatter away from the jammer and the transition bands of the filters become narrower for the higher order cases.

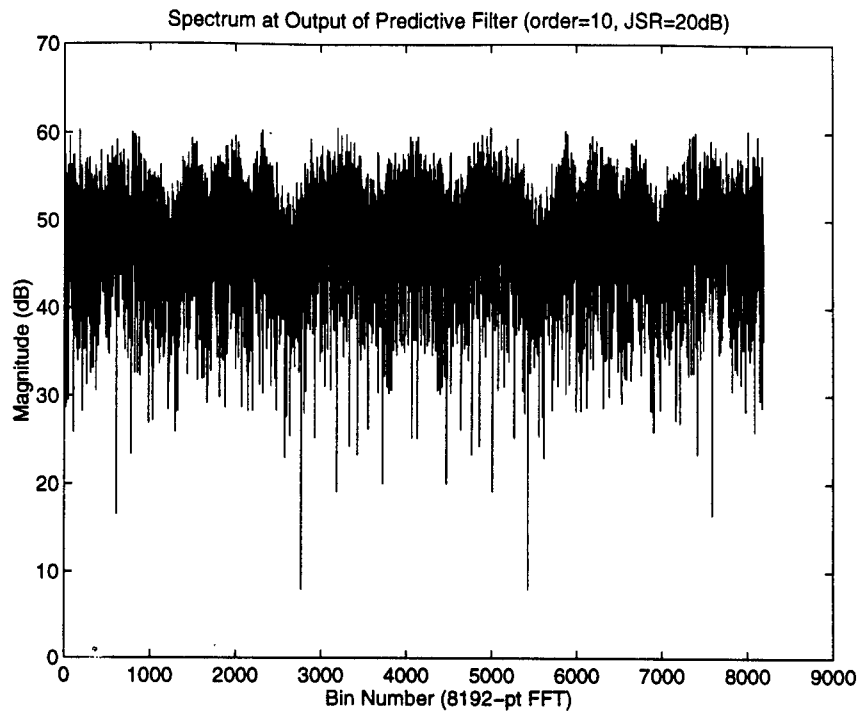


Figure 3.3: Output spectrum for the predictive filter.

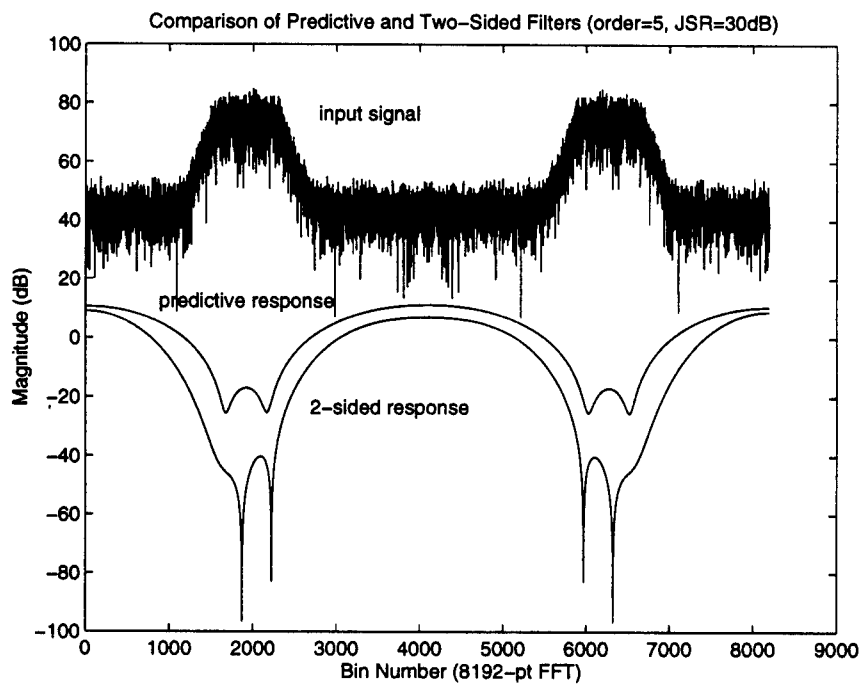


Figure 3.4: Comparison of frequency responses for order = 5, JSR = 30 dB.

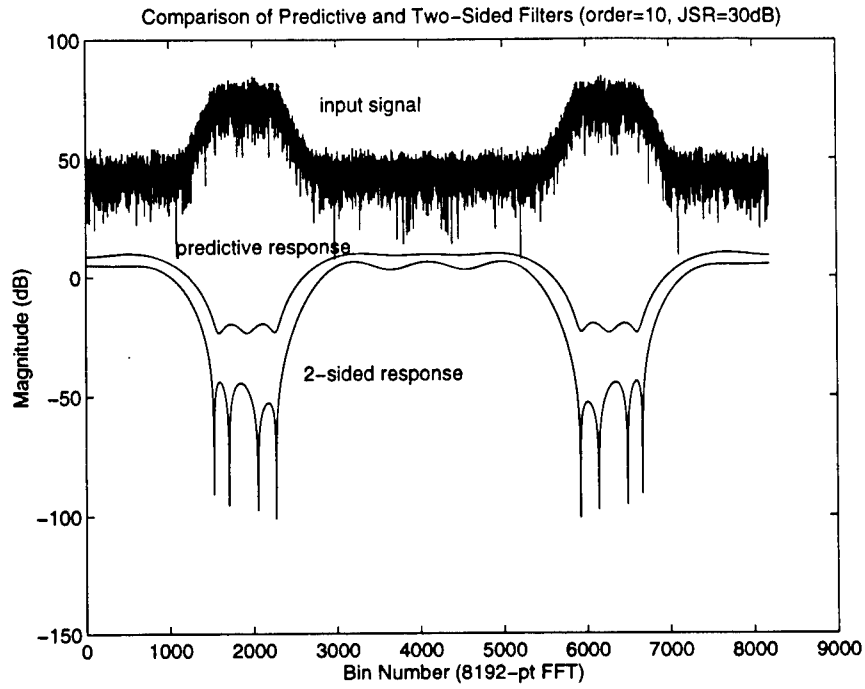


Figure 3.5: Comparison of frequency responses for order = 10, JSR = 30 dB.

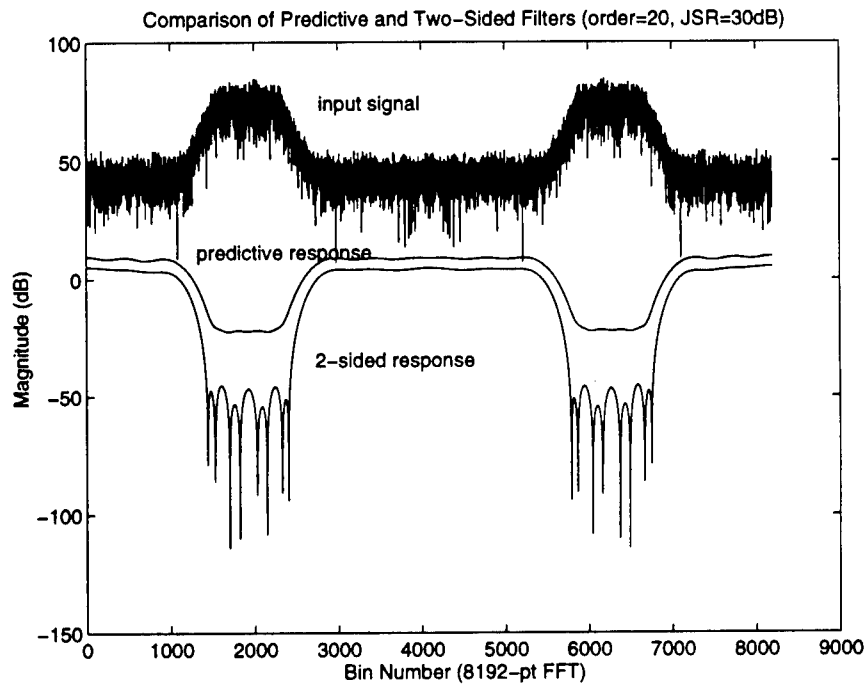


Figure 3.6: Comparison of frequency responses for order = 20, JSR = 30 dB.

Chapter 4

Filter Compensation

When a signal passes through a multipath channel, very often the receiver will incorporate some type of *equalization* or *compensation* process to mitigate the effects of the channel. With spread spectrum signaling, this equalization is usually performed using a RAKE receiver [10, 11], which seeks to coherently combine the signal energy contained in the multiple delayed signal copies. For the case where the transmit signal bandwidth exceeds the coherence bandwidth of the channel, the fading is said to be *frequency selective* and the channel is often modeled as a tapped delay line structure as shown in Figure 4.1. In this case, it is

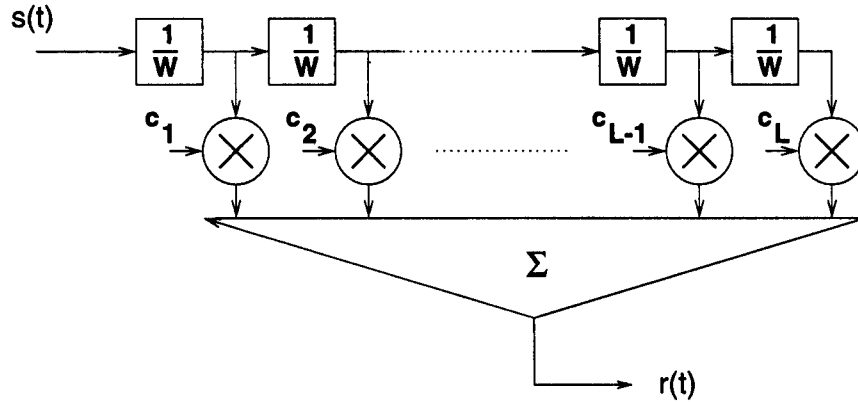


Figure 4.1: Tapped delay line channel model.

assumed that the RF bandwidth of the signal is W , and the channel model consists of complex channel coefficients, c_1, c_2, \dots, c_L which are spaced in time by $1/W$. The tap weights are time varying, resulting in a channel frequency response that is time varying. A RAKE receiver uses knowledge of the channel response, i.e. knowledge of c_1, c_2, \dots, c_L to perform the compensation process. One form of the RAKE receiver is shown in Figure 4.2. The receiver consists of a tapped delay line structure with the same tap spacing as the channel.

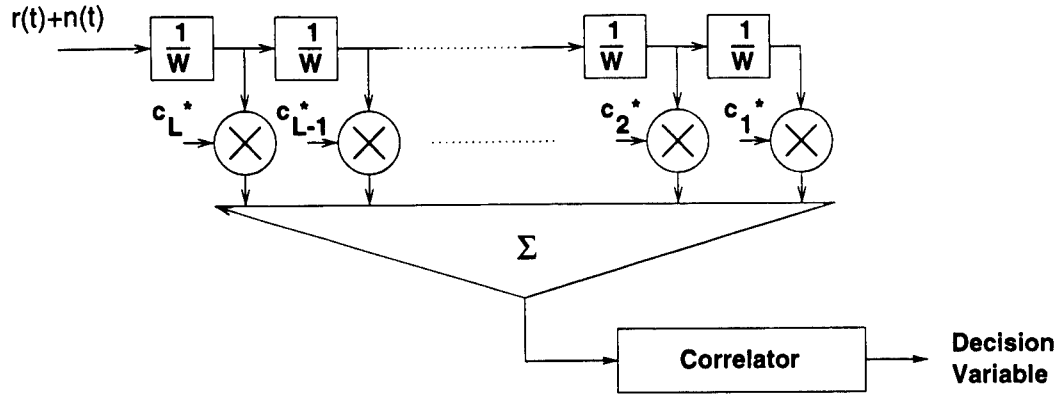


Figure 4.2: One form of the RAKE receiver.

The tap weights, however, are time reversed and complex conjugated with respect to those of the channel. The output of the tapped delay filter is fed to a standard correlator receiver which despreads the spread spectrum signal and produces the decision variable.

The operation, and optimality, of the receiver is easy to understand. Assume that the DSSS signal is produced by feeding impulses, with amplitude ± 1 depending on the particular data bit being sent, into a FIR filter having a impulse response that is equal to the spreading sequence. The output of this filter passes through a second filter that produces the multipath channel effects and the output of this filter is summed with white Gaussian noise and fed to the receiver. For optimal detection of a signal in AWGN, the received signal should be processed by a *matched filter*, which has an impulse response that is the time-reversed, complex conjugated version of the signal. In this case, the receive filter must be matched to the cascade of the spreading and channel filters. The RAKE receiver makes this receive filter as a cascade, one filter matched to the channel and a second, the correlator, matched to the spreading filter. The result is optimal detection in AWGN.

The concept behind the adaptive filter compensation technique is to view the adaptive filter suppressor as a *known* multipath channel and follow it by a RAKE receiver to compensate for the distortion that it introduces. In the case of the predictive filter, the channel has the coefficients $1, -w_1, -w_2, \dots, -w_N$ while, in the case of the two-sided filter, the coefficients are $-w_N, \dots, -w_1, 1, -w_1, \dots, -w_N$.

Figure 4.3 shows the structure of the compensated adaptive filter receiver. The tap weights from the adaptive suppressor are fed forward to the RAKE combiner which uses them to compensate or equalize the multipath distortion produced in the interference suppression process. For this case, the tap spacing in the RAKE is the same as that in the adaptive suppressor and is equal to one chip interval. The output of the RAKE combiner is then processed by a correlator matched the spreading code.

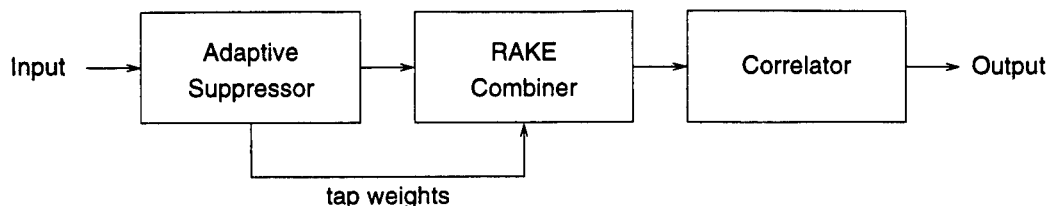


Figure 4.3: Compensated adaptive filter receiver.

For this receiver to be optimal, it is necessary for the DSSS signal to be in AWGN at the output of the adaptive filter, since the operation of the RAKE is predicated upon the signal being contained in AWGN. If we consider the predictive filter which, as shown earlier, acts as a pre-whitener, this condition is approximately met. First assume that the power spectral density (PSD) of the DSSS signal is flat, i.e. that the DSSS signal is white, and that there is a significant amount of processing gain such that the PSD of the AWGN is significantly larger than that of the nearly white DSSS signal at the input to the adaptive filter. The signal at the output of the adaptive filter consists of the sum of filtered DSSS, AWGN and interference terms and this composite signal has a flat frequency spectrum. If there is a strong narrowband interference term at the input of the adaptive filter, then the adaptive filter will adjust its frequency response to suppress the portion of the band occupied by the narrowband interference in order to make the output spectrum white. Since the PSD of the AWGN is significantly larger than that of the DSSS signal, the *PSD of the sum of the filtered AWGN and interference is approximately white*. If the interference is a narrowband Gaussian process, then the sum of the filtered AWGN and interference will clearly be Gaussian; if the interference is not Gaussian, e.g. a tone, then the sum will likely be approximately Gaussian because the sum is dominated by the AWGN. Under these approximations, then, the input to the RAKE can be considered to be the DSSS signal distorted by the transfer function of the adaptive filter suppressor in AWGN.

For the two-sided filter, the same reasoning cannot be used since the filter acts as a power inverter. In this case the compensation process is not optimal or even nearly optimal and, in fact, serves only to worsen the performance. As will be demonstrated later, the two-sided filter actually develops a frequency response that approximates the cascade of the predictive filter and the RAKE combiner, effectively producing the compensated system in one stage.

Chapter 5

SPW Simulation

The systems were modeled in SPW to allow study of their behavior and performance. The sections below describe the simulation systems. To simplify the implementation, all functions were implemented for real rather than complex signals. It is assumed in the simulations that perfect carrier and chip synchronization is maintained. Under these conditions and with BPSK signaling, the use of real signal does not result in any loss of accuracy in the model.

5.1 Test Signal Generation

The performance of the adaptive filters will be studied when the input signal consists of a DSSS signal with AWGN and either single tone jamming or narrowband Gaussian jamming. In all cases the DSSS signal will be generated using a 63-chip pseudo-noise (PN) signal with the data bit duration equal to the duration of a full length of the code. The signal is sampled once per chip. The narrowband Gaussian jammer is generated by passing the output of a Gaussian noise source through a 10th order Butterworth bandpass filter with a variable 3 dB bandwidth and center frequency. Figure 5.1 shows the SPW implementation of the signal generation system along with the selectable parameters.

5.2 Adaptive Filters

The predictive adaptive filter suppressor is implemented using the adaptive filter block provided by SPW. This provided block is configured such that the reference input, i.e. the input to the delay line, is operated upon by the first tap weight *before* being delayed. This is contrary to the required configuration that is shown in Figure 2.1 where the reference

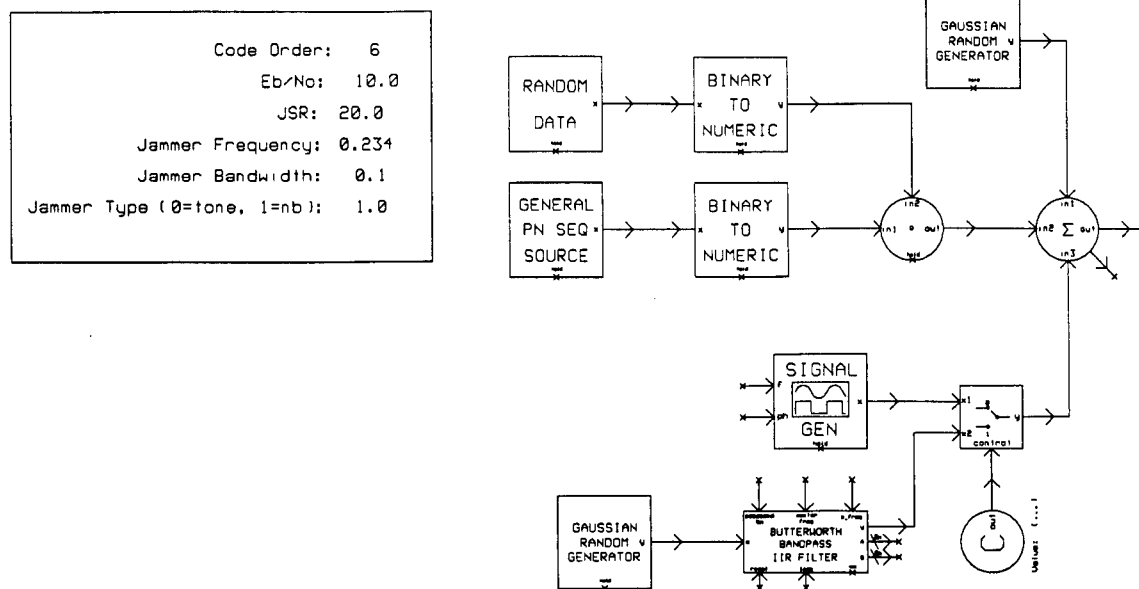


Figure 5.1: Signal Generation in SPW

input is first delayed before being multiplied by the first tap weight. As a consequence, the predictive filter suppressor is constructed by adding an additional delay in the reference input path, as shown in Figure 5.2.

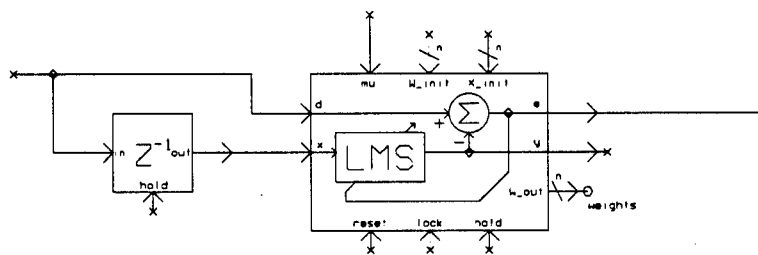


Figure 5.2: Predictive adaptive filter suppressor.

The two-sided filter is implemented using two of the adaptive filter blocks provided by SPW and is shown in Figure 5.3. The adaptive weights on each side of the filter are implemented using an adaptive filter block and the center, unity-valued tap is wired into the diagram. As implemented, this system does not force the tap weights on each side of the filter to be mirror images of each other though, in practice, they adapt to produce this condition.

Figure 5.4 shows the structure used to implement the compensated predictive adaptive suppressor. In this case the tap weights from the predictive filter are time-reversed and used

Two-sided LMS Adaptive Filter with Inputs Tied Together

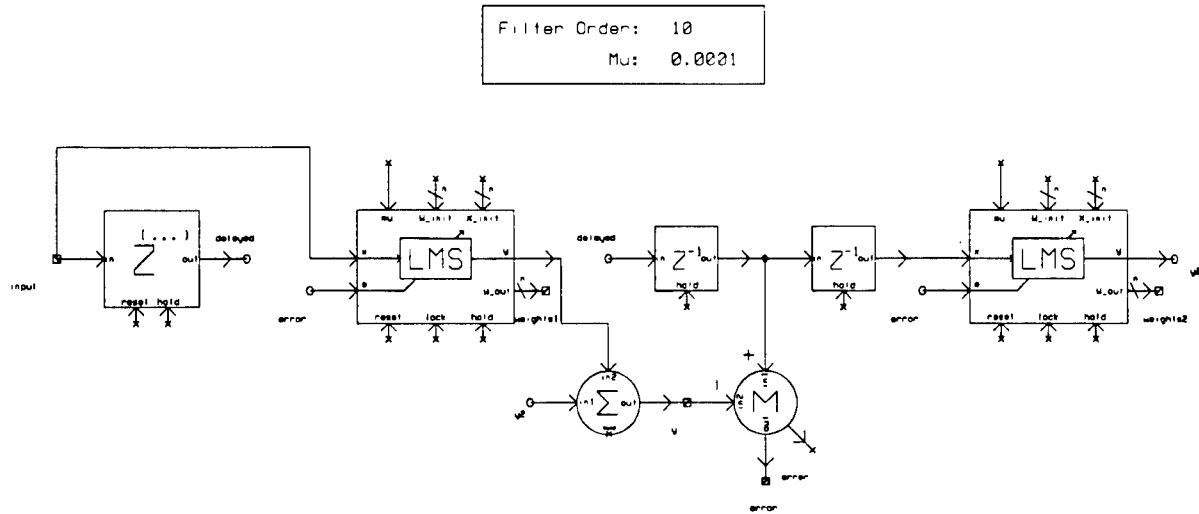


Figure 5.3: Two-sided adaptive filter suppressor.

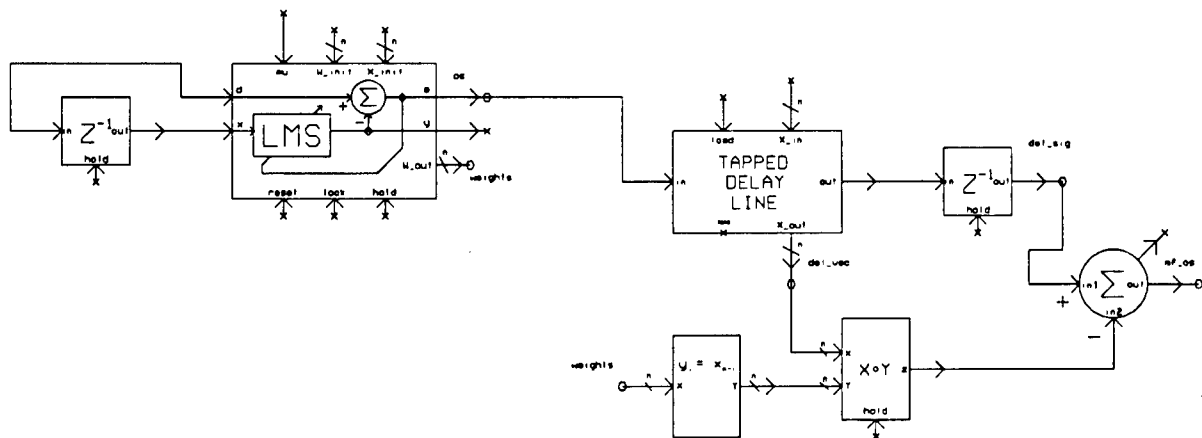


Figure 5.4: Compensated predictive adaptive filter suppressor.

in the RAKE combiner. Since the signals and filter tap weights are real-valued, complex conjugation is not required. Figure 5.5 shows the structure of the compensated two-sided adaptive filter suppressor. The structure closely parallels that of the compensated predictive

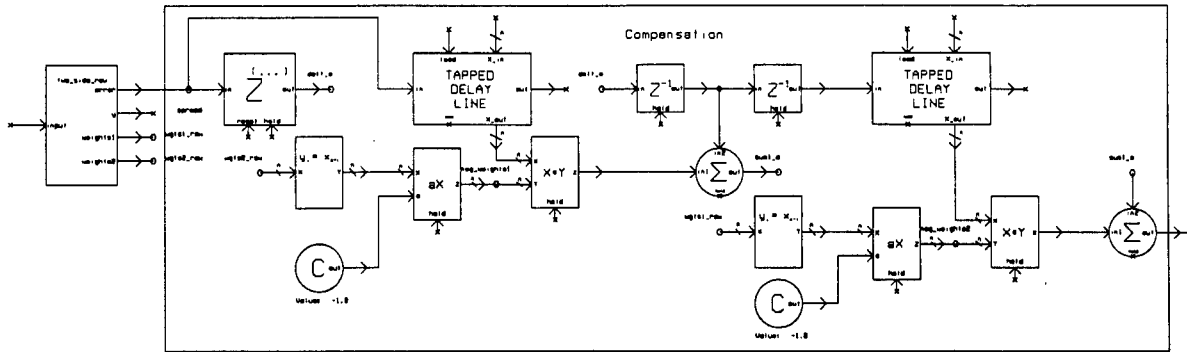


Figure 5.5: Compensated two-sided adaptive filter suppressor.

filter. The two-sided adaptive filter itself, previously shown in Figure 5.3, is contained in the block on the left and the remainder of the structure simply implements the same filter with the tap weights reversed. Due to the symmetry in the two-sided filter, the filter with the tap weights reversed is actually the identical filter.

5.3 Test Systems

Many different test systems were constructed using the building blocks described above. In all cases, the despreading operation was performed using vector operations, where the unmodulated PN sequence and the spread information-bearing signal, obtained directly from the channel, the output of an adaptive suppressor or the output of a compensated adaptive suppressor, are converted to vectors and processed using a dot multiply to produce a scalar decision variable. In constructing the vectors, care is taken to ensure that each vector, which has a length equal to the number of chips in the PN sequence which also equals the processing gain of the system, contains a segment of the signal that is aligned with the start and end of the PN sequence.

Systems were created to investigate the following:

- Determine the BER performance of the compensated and uncompensated adaptive filter systems.
- Determine the make-up of the signal after suppression, i.e. the effect of residual interference power vs. the effect of the code distortion on the BER performance of the system.

This second case is handled by creating a system which implements copies of the adaptive suppressor whose weights are determined by one master suppressor. What this means is that the composite DSSS signal, AWGN and interference signal is fed into an adaptive suppressor which adjusts its tap weights in an attempt to remove the interference. The tap weights are then copied to non-adaptive filters which implement the same structure but which are fed individual components of the input signal, i.e. the DSSS signal alone, the AWGN alone or the interference alone, rather than the composite signal. Since the systems are linear, summing the outputs of these filter would produce the same signal as from the adaptive suppressor. However, by generating the components separately, it is possible to see how the individual components are affected by the suppression process.

Chapter 6

Performance Results

The BER performance of the adaptive filter receivers, both with and without compensation, were evaluated using SPW. Some of the main properties of the simulations are given below.

- Spreading is performed with one data bit per length of the PN sequence, where the sequence length is 63.
- Results are obtained using Monte Carlo simulation with a minimum of 200 errors for each data point.
- Modulation is BPSK with the channel modeled at baseband.
- Perfect carrier, chip and data synchronization is assumed.
- AWGN and narrowband interference are introduced in the channel. The narrowband interference is either a single tone or narrowband Gaussian waveform.

The sections below show some performance results first for a channel with AWGN and interference and then for a channel with multipath propagation.

6.1 AWGN and Interference

Figure 6.1 shows the performance of the various systems as a function of the bit energy to one-sided noise power spectral density, E_b/N_o for a single tone jammer with a normalized frequency of 0.234 and a JSR of 20 dB. The order of the adaptive suppressors is 10. The figure shows the performance of both the predictive and two-sided filters both with and

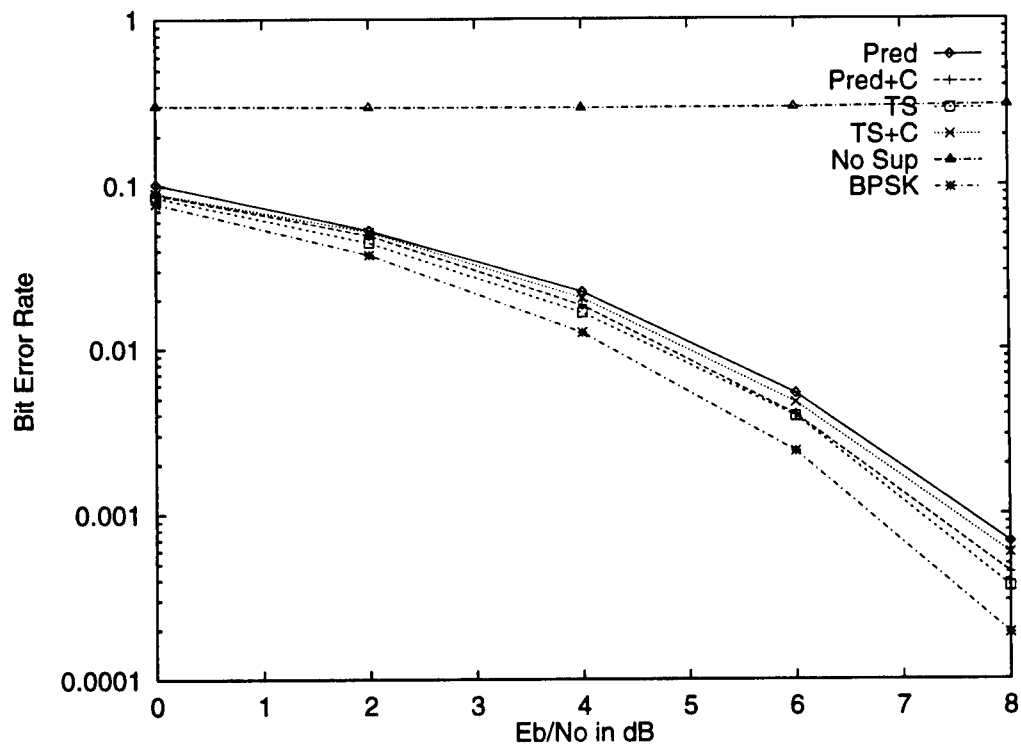


Figure 6.1: BER vs. E_b/N_o for a single tone jammer with frequency = 0.234 and JSR = 20 dB. Filter order = 10.

without compensation along with the performance without any interference suppression (No Sup) and the performance in AWGN alone (BPSK) calculated using

$$\text{BER} = \frac{1}{2} \text{erfc} \left[\sqrt{\frac{E_b}{N_o}} \right] \quad (6.1)$$

where $\text{erfc}(x)$ is the complementary error function given by

$$\text{erfc}(x) = \frac{2}{\sqrt{\pi}} \int_x^{\infty} e^{-t^2} dt \quad (6.2)$$

Each of the suppressors provide a large improvement in performance over the no suppression case. The predictive filter is the worst of the suppressors while the two-sided filter and the compensated predictive filter provide the best performance. The compensated two-sided filter does not provide performance that is as good as the two-sided filter alone. This results is not surprising since the compensated two-sided filter is clearly not an optimal receiver configuration.

A greater spread in performance is obtained with the use of a narrowband Gaussian jammer. Figure 6.2 shows the performance of the various systems as a function of E_b/N_o for a narrowband Gaussian jammer having a JSR of 20 dB, normalized center frequency of 0.237 and a normalized bandwidth of 0.1. The order of the adaptive suppressors is 20.

The curves clearly show that the predictive filter alone (Pred) is the least effective of the suppressors. The performance of the compensated predictive filter (Pred + C) and the two-sided filter (TS) are virtually identical. As will be shown later, this is because the two structures implement nearly the identical transfer function. The compensated two-sided filter (TS + C) actually performs *worse* than the two-sided filter alone.

Figure 6.3 shows the results for the same jammer when the filter order is reduced to 10. Very little performance degradation is evident in the figure. To investigate this point further, Figure 6.4 shows how the BER varies with the filter order for this same jammer when E_b/N_o is fixed at 6 dB. Due to the fact that the compensated two-side filter does not perform as well as the two-sided filter alone, performance results are not provided for it on the figure. As the figure shows, once the order gets above approximately 7, the performance remains relatively constant for further increases.

Figure 6.5 shows how the BER performance varies as a function of the jammer bandwidth. For this case, the jammer frequency is 0.234 and JSR = 20 dB. The figure shows the performance without suppression, with the predictive adaptive filter, with the two-sided adaptive filter and an "ideal" performance. The ideal performance is derived assuming that the portion of the bandwidth of the signal that overlaps the jammer is lost along with all the jammer energy during the suppression process. Consequently, if the jammer bandwidth is 0.1, the performance is calculated assuming that 20% of the signal energy is loss. The actual bandwidth affected by the jammer is twice the bandwidth of the jammer due to

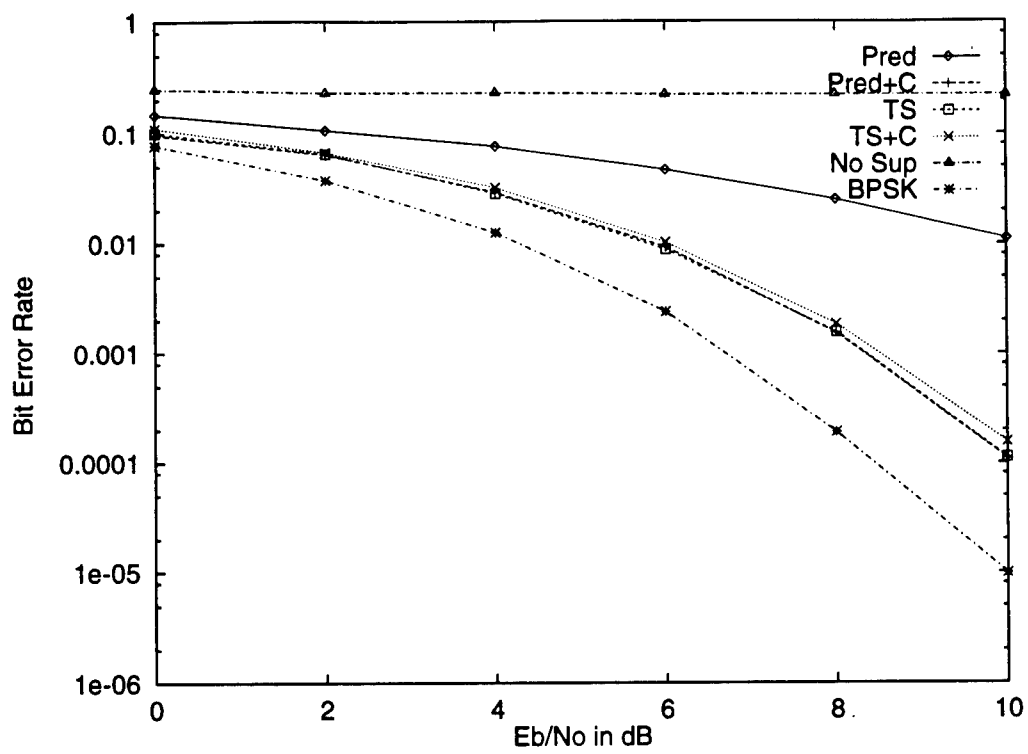


Figure 6.2: BER vs. E_b/N_o for a narrowband Gaussian jammer with frequency 0.234 and bandwidth 0.1. Filter order = 20.

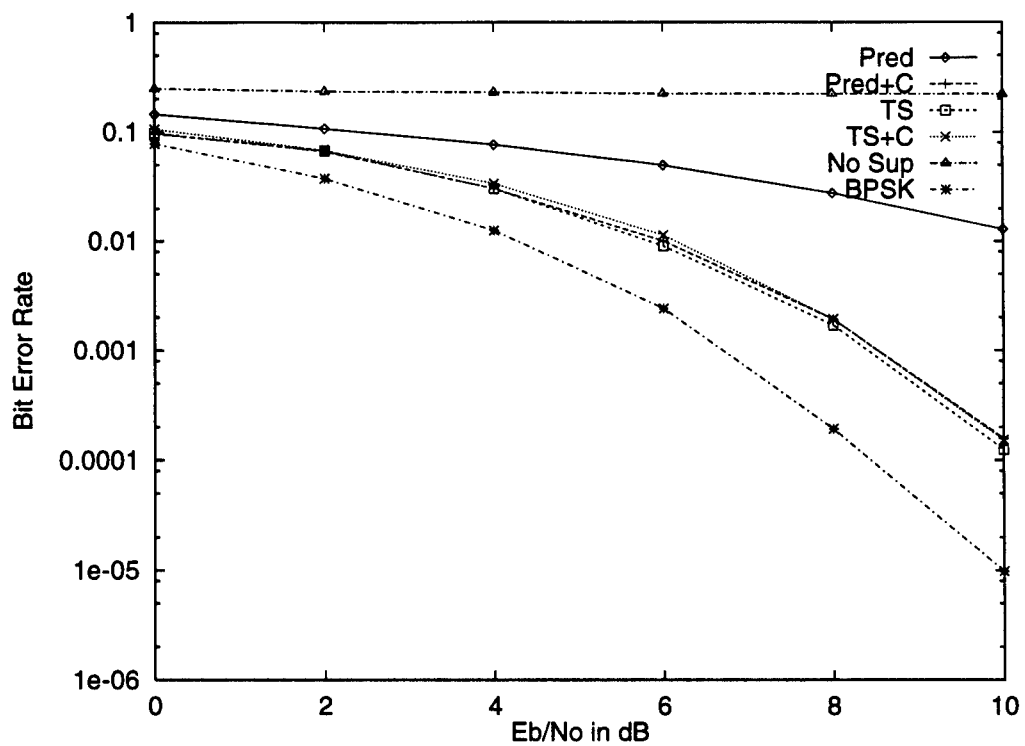


Figure 6.3: BER vs. E_b/N_o for a narrowband Gaussian jammer with frequency 0.234 and bandwidth 0.1. Filter order = 10.

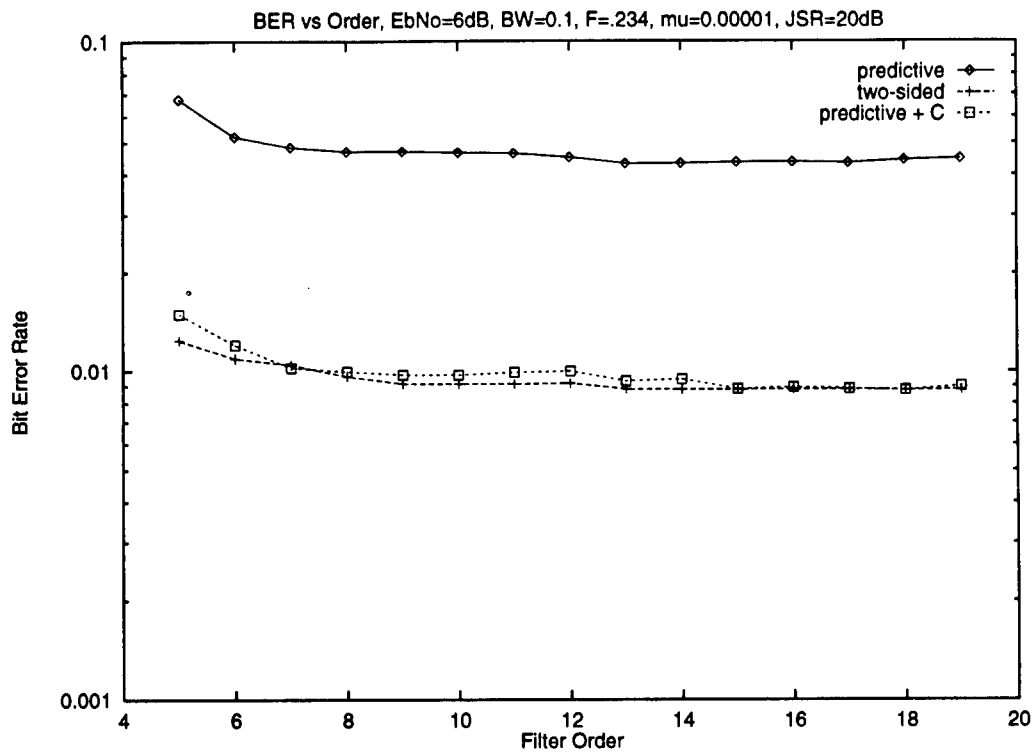


Figure 6.4: BER vs. filter order for a narrowband Gaussian jammer with frequency 0.234 and bandwidth 0.1. $E_b/N_o = 6$ dB.

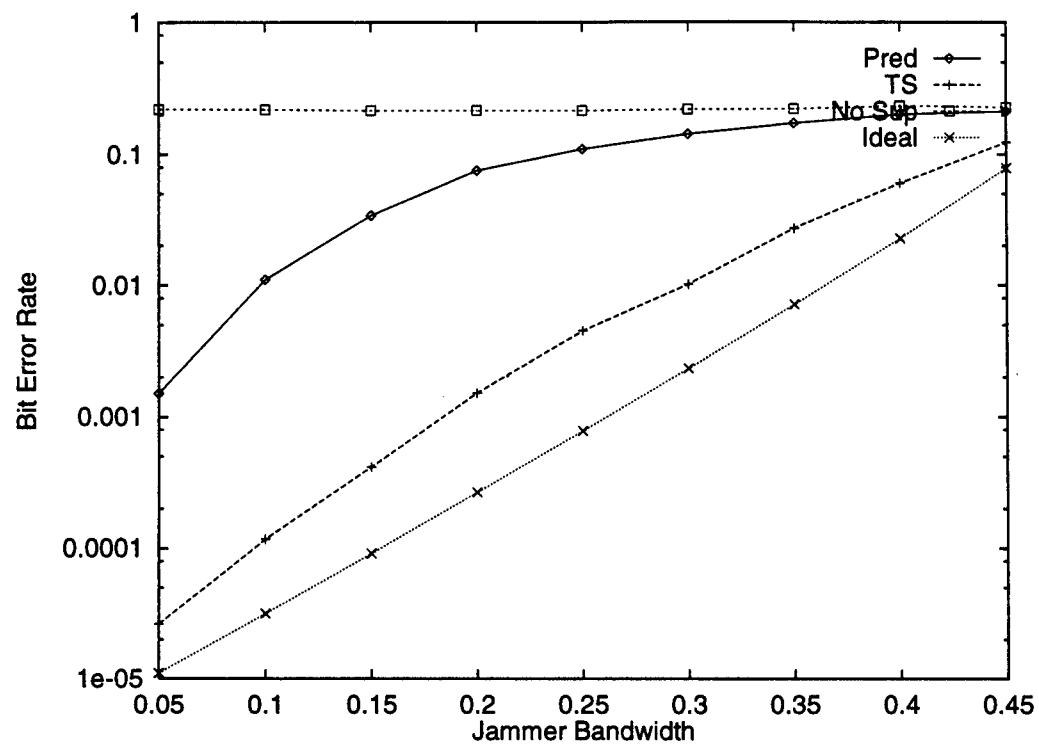


Figure 6.5: BER vs: jammer bandwidth for a narrowband Gaussian jammer with frequency 0.234 and JSR = 20 dB. $E_b/N_o = 10$ dB.

aliasing, as demonstrated in Section 3.2. Under this simple assumption, the BER can be calculated in the following way. First,

$$(E_b/N_o)_{\text{sup}} = (E_b/N_o)[1 - 2(BW)], \quad (6.3)$$

where $(E_b/N_o)_{\text{sup}}$ is the value of E_b/N_o after suppression and BW is the bandwidth of the narrowband Gaussian jammer. To determine BER, the result of (6.3) is inserted into (6.1).

Figure 6.5 shows that the performance of the two-sided filter remains much better than that of the predictive filter as the bandwidth increases. The performance of the two-sided filter is also near the ideal performance. It is not expected that the two-sided performance should be equal to the ideal performance since the ideal performance does not account for the residual jammer energy, the code distortion or the finite transition bands of the filter.

In order to explore the issue of the variation of the two-sided performance from the ideal performance, a simulation was configured to determine how much performance loss is the result of residual jammer energy in the output of the adaptive suppressor. As described in Section 5.3, this simulation used replicas of the suppression filter to process the interference, noise and spreading sequence separately, allowing the effect of each component to be isolated from that of the others. Tap weights are still determined based on the composite signal, however. Figure 6.6 shows some results from this simulation. Of primary interest in the figure are the three curves which represent the performance of the two-sided filter for a signal consisting of the spread spectrum signal, noise and interference (TS), the performance for the two-sided filter for a signal consisting of the spread spectrum signal and noise only (TS/Noise Only), and the ideal performance (Ideal) determined by (6.3) and (6.1). Note that the removal of the interference component has little effect on the BER, indicating that there is very little residual interference energy at the output of the filter. Note also that the ideal performance, which considers only the loss of spread spectrum signal energy due to the removal of a portion of the band, is near the other curves, indicating that the primary source of performance loss relative to the theoretical BPSK performance is due the loss of spread spectrum signal energy.

As demonstrated by the BER results, the compensated predictive filter and the two-sided filter have nearly identical performance. To demonstrate the equivalence of the two structures, **Matlab** was used to generate the tap weights for both filters with a narrowband Gaussian jammer having JSR = 30 dB and a bandwidth of 0.1. Additionally, the compensation for the predictive filter was implemented by convolving the impulse response of the predictive filter with the time reverse of itself, producing the impulse response of the cascade of the predictive filter and its matched filter. Figure 6.7 shows the impulse responses for the two-sided filter and the compensated predictive filters overlayed. As is evident in the figure, the impulse responses are nearly identical except for the very edges. One reason for this variation is that the tap weights for the two-sided filter use knowledge of a broader range of autocorrelation values. Figure 6.8 shows the frequency responses of the two structures, obtained by taking the FFT of each of the impulse responses in Figure 6.7.

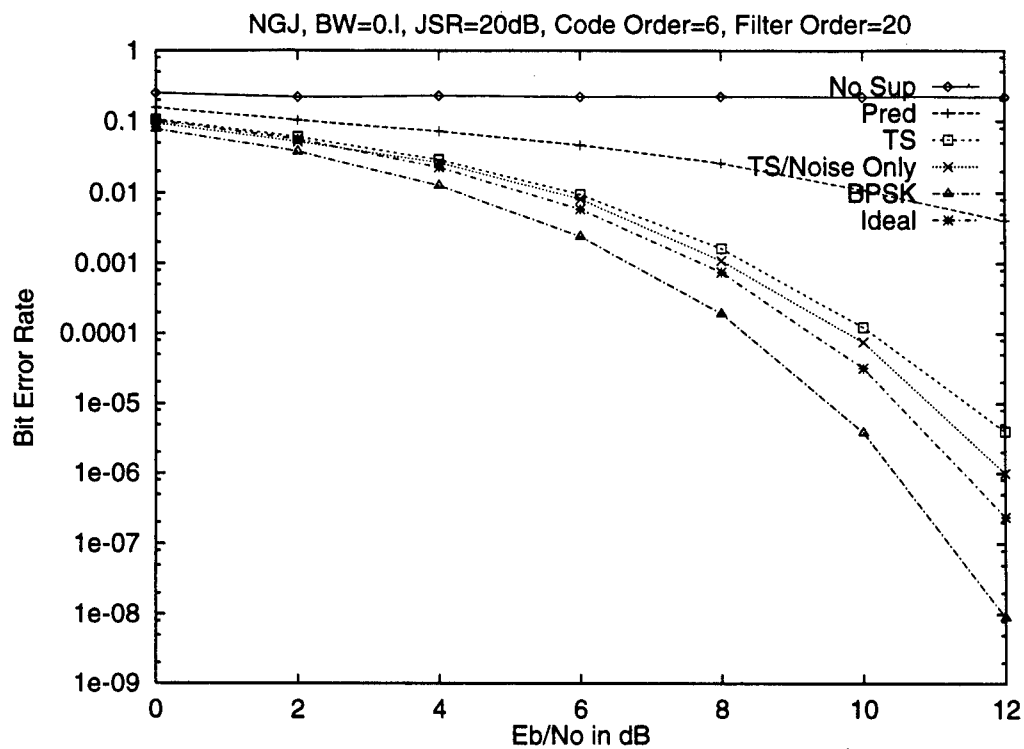


Figure 6.6: BER vs. E_b/N_o for a narrowband Gaussian jammer with frequency 0.234, bandwidth = 0.1 and JSR = 20 dB. Included is the result when the residual jammer energy is removed from the output.

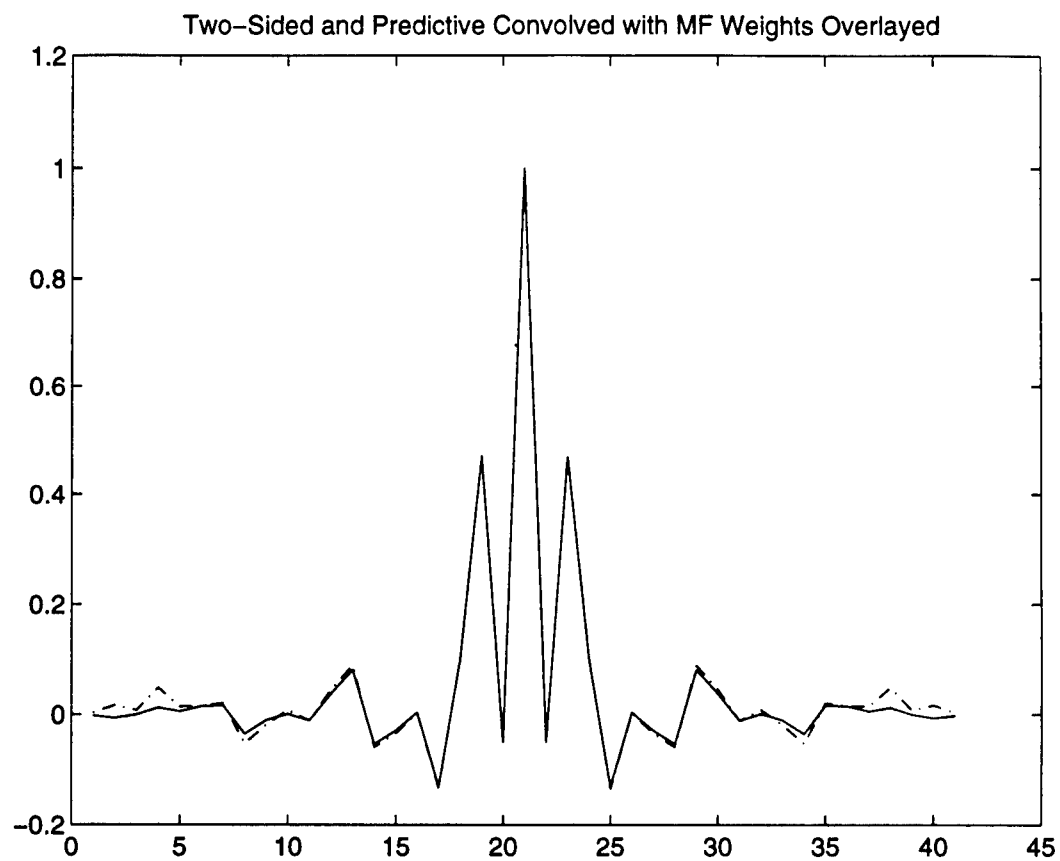


Figure 6.7: Overlay of the impulse responses of the compensated predictive filter (dashed) and the two-sided filter (solid). $E_b/N_o=10$ dB, JSR = 30 dB, frequency = 0.234 and bandwidth = 0.1.

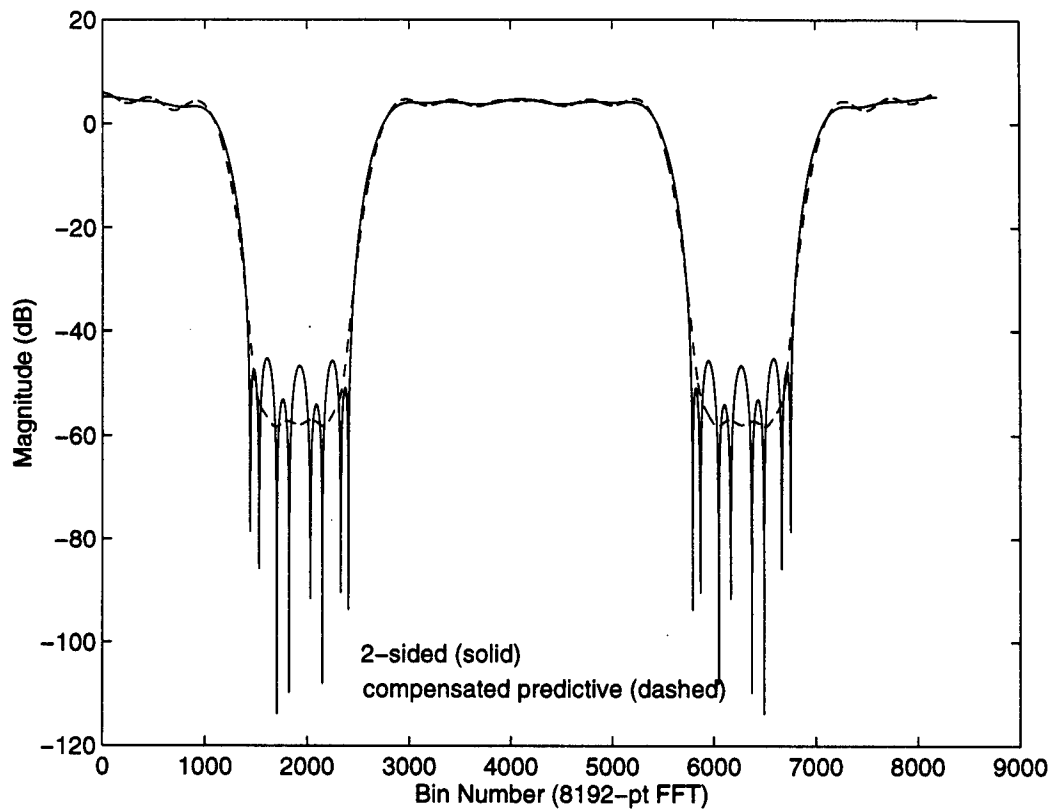


Figure 6.8: Overlay of the frequency responses of the compensated predictive filter (dashed) and the two-sided filter (solid). $E_b/N_o=10$ dB, JSR = 30 dB, frequency = 0.234 and bandwidth = 0.1.

responses of Figure 6.7. The frequency responses again show that the two structures are nearly equivalent. The primary difference between the responses is the greater suppression provided by the compensated predictive filter, though the effect of this additional suppression on BER performance is negligible. The two responses are very nearly the same away from the suppression region.

6.2 Multipath Channel

Very often the channel will be characterized by multipath propagation in addition to AWGN and interference. As a result, it is important to study how the interference suppression techniques, in this case the predictive and two-sided adaptive filters, react to the presence of multiple delayed copies of the DSSS signal in the received signal. To this end, a simulation was configured which models a static two-path channel, producing two equal-power copies of the DSSS signal separated in time by two chips. In all cases the value of E_b/N_o **does not** take into account the extra energy in the second path. As a result, if the receiver ignores the second ray, the performance should ideally follow the theoretical BPSK performance. However, if the receiver is able to use the energy in the second ray in a constructive manner, the performance could potentially be 3 dB to the **left** of the theoretical BPSK performance.

Figure 6.9 shows how the introduction of the two-ray multipath channel affects the performance of the predictive filter. The figure shows the performance without suppression (No Sup) as well as with the predictive filter (Pred) both with and without multipath (MP and No MP, respectively). Since all the curves are very near the theoretical BPSK in AWGN performance (the no suppression, no multipath case lies on top of the theoretical curve), the results indicate the the presence of multipath results in only a very small degradation in both the no suppression and predictive filter cases. The reason for this behavior is that the despreading is performed using a copy of the spreading sequence that is synchronized with the multipath ray with the least delay, making the adaptive filter unable to use the correlation introduced by the multipath to cancel part of the code.

In contrast, the two-sided filter uses both past and future samples when predicting the current sample meaning that it should have problems with the multipath channel. Figure 6.10 shows performance results for this case. It is clear that the two-sided adaptive filter is suppressing some of the DSSS signal, resulting in an increase in the BER. The presence of the multipath has introduced correlation between the DSSS portion of the received signal and it was the lack of this correlation that gave the two-sided filter its ability to selectively suppress the interference and not the DSSS signal.

The next few figures examine the behavior of the adaptive suppressors for a channel that contains both multipath and interference. Figure 6.11 compares the performance of the predictive filter for multipath and no multipath channels when a narrowband Gaussian

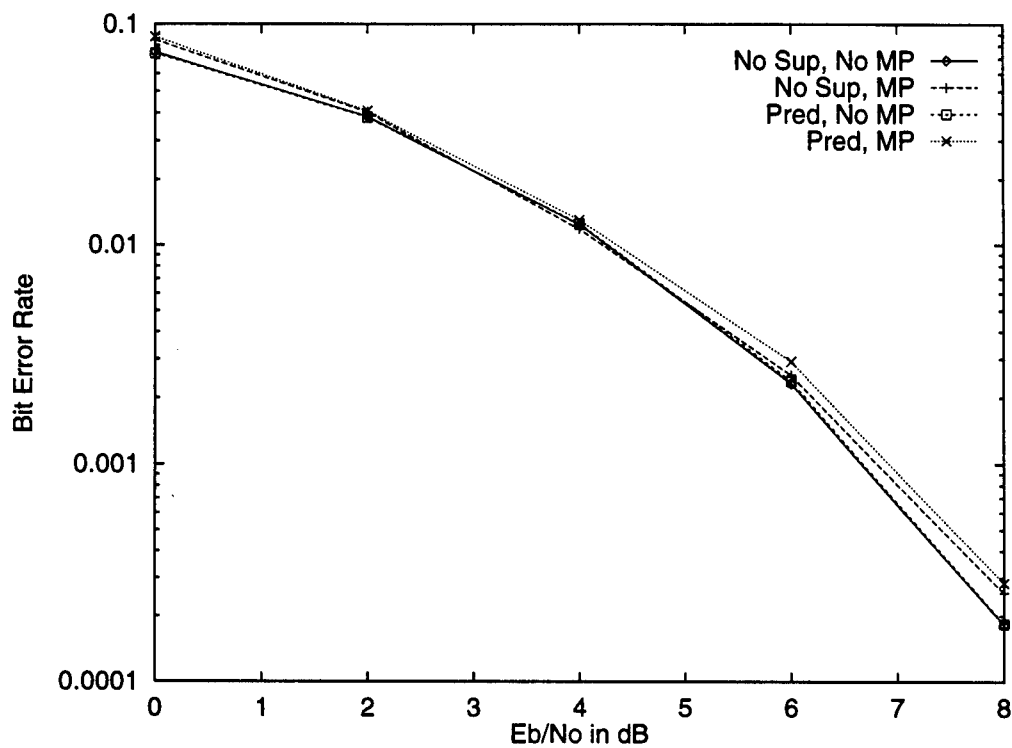


Figure 6.9: BER performance of the predictive adaptive suppressor with a two-ray multipath channel and no interference.

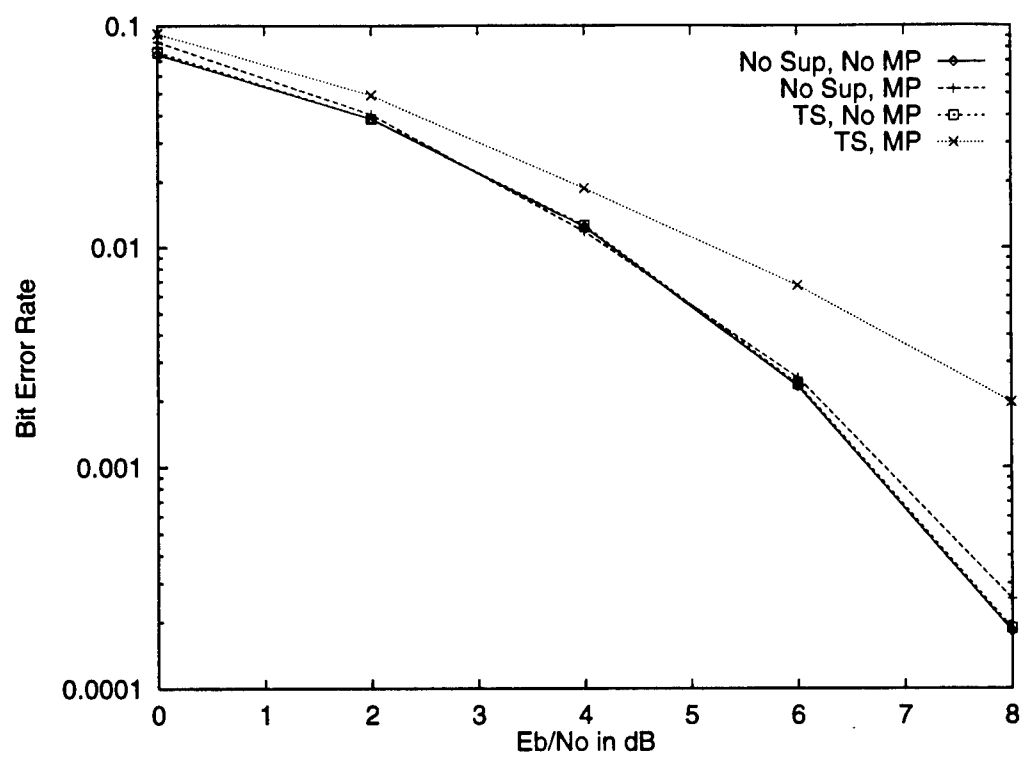


Figure 6.10: BER performance of the two-sided adaptive suppressor with a two-ray multi-path channel and no interference.

jammer with frequency of 0.234, bandwidth of 0.1 and JSR of 20 dB is present. As in the earlier results for the predictive filter, there is only a slight degradation in performance due to the multipath. Figure 6.12 shows the results for the two-sided filter both with and without multipath. Here the results are much different because the presence of multipath actually *improves* the performance of the receiver. The BER curve for the case with interference and multipath falls to the left of the theoretical BPSK curve, indicating that the adaptive suppressor is able to use the energy in the second path.

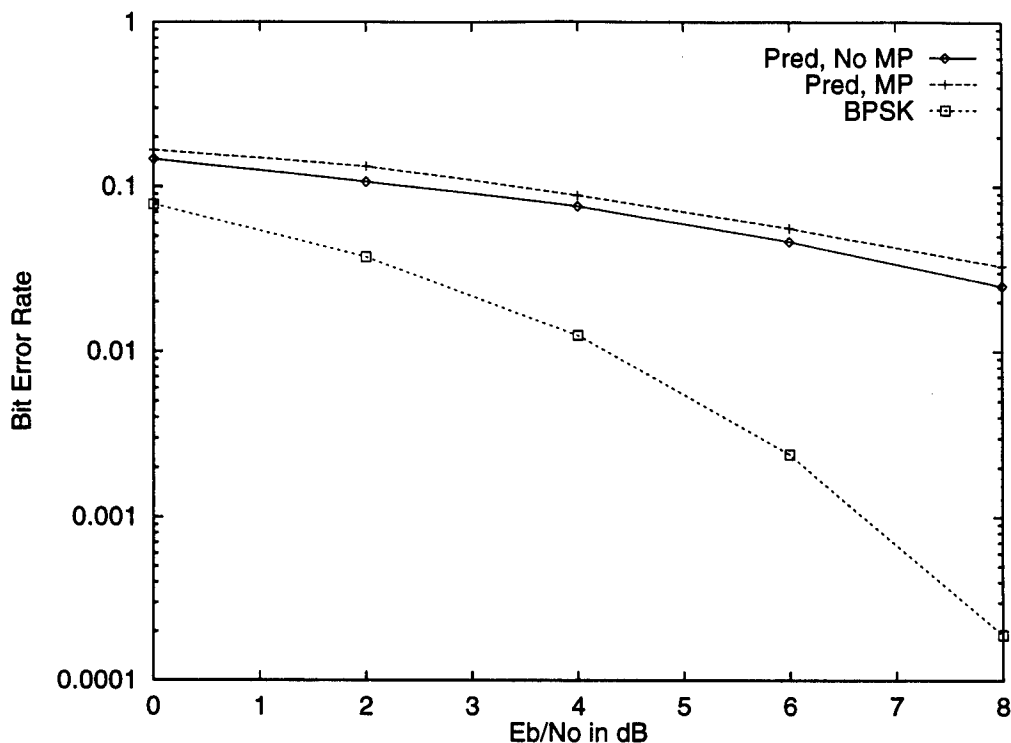


Figure 6.11: BER performance of the predictive adaptive suppressor with a two-ray multipath channel and interference. Interference frequency = 0.234, bandwidth = 0.1 and JSR = 20 dB.

The improvement in performance with multipath that is evident in Figure 6.12 appears to be due to a special, and unusual, combination of interference and multipath. Figure 6.13 shows the results for both the predictive and two-sided adaptive filters when the interference frequency is moved to 0.1176. In this more typical case, the results for the two-sided filter show the expected degradation with the addition of the multipath.

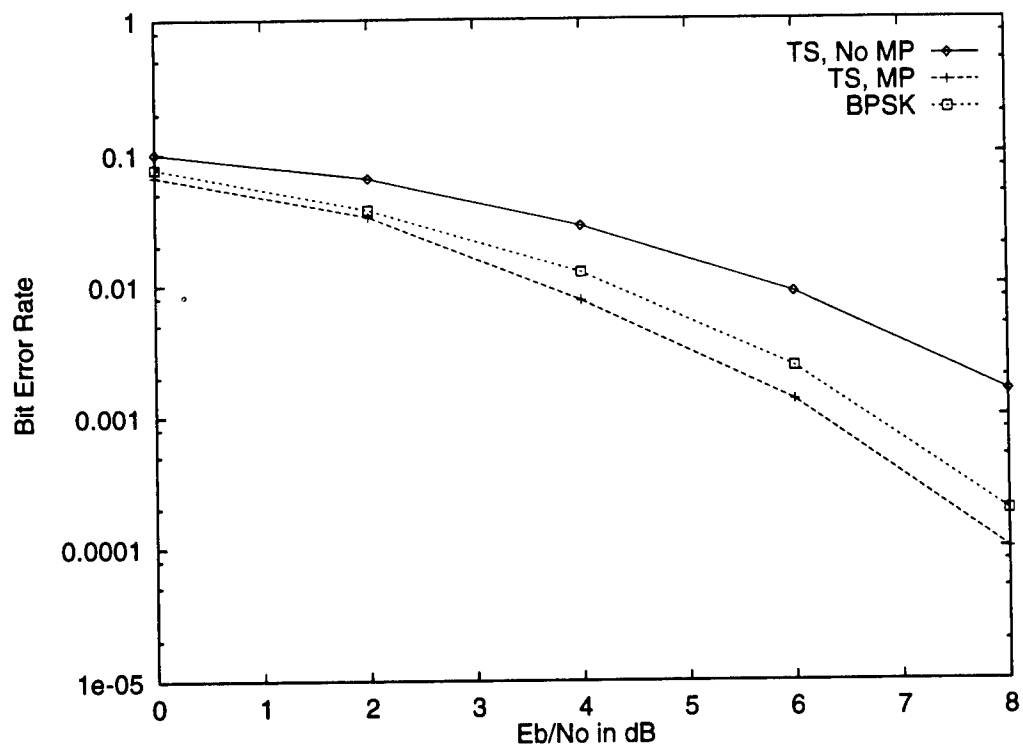


Figure 6.12: BER performance of the two-sided adaptive suppressor with a two-ray multi-path channel and interference. Interference frequency = 0.234, bandwidth = 0.1 and JSR = 20 dB.

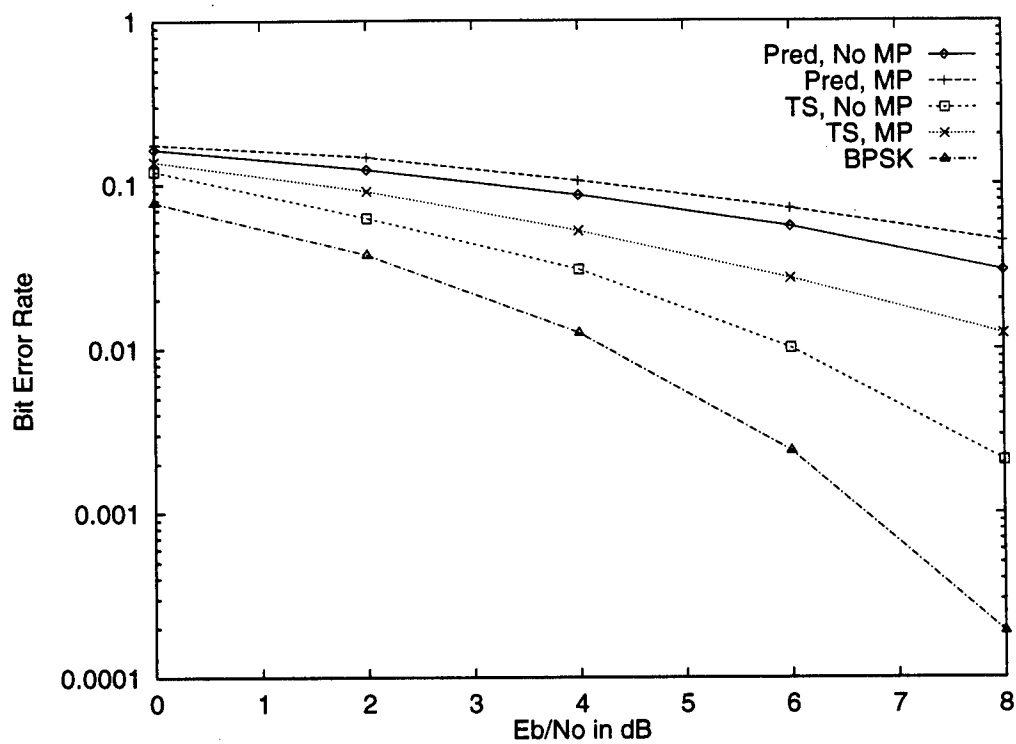


Figure 6.13: BER performance of the predictive and two-sided adaptive suppressors with a two-ray multipath channel and interference. Interference frequency = 0.1176, bandwidth = 0.1 and JSR = 20 dB.

Chapter 7

Summary and Conclusions

The following tasks were accomplished during this effort:

- Simulations were developed in the Signal Processing WorkSystem (SPW) from Alta-Group of Cadence Designs for direct sequence spread spectrum systems for a channel with tone and narrowband Gaussian interference and AWGN. Receivers have been implemented which use both the predictive and two-sided adaptive filter interference suppressors as well as a compensation technique which attempts to remove the code distortion introduced in the interference suppression process.
- Analytical results were obtained which provide the tap weights for both the predictive and two-sided filters given the auto-correlation of the input signal.
- We studied the improvement provided by the compensation technique for tone and narrowband Gaussian interference.
- We studied the source of the remaining performance loss, relative the performance in AWGN alone, after adaptive suppression of narrowband Gaussian interference .
- We investigated how the presence of multipath propagation in the channel affects the performance of the adaptive suppressors.

Based on the above accomplishments, we can conclude the following:

- The compensation technique provides a large performance improvement for the predictive filter but does not provide any performance improvement for the two-sided filter.
- The predictive filter alone acts as a pre-whitener while the two-sided filter alone acts as a power-inverter.

- The two-sided filter is equivalent to the compensated predictive filter. In other words, the predictive filter cascaded with the compensating filter has the same impulse response as the two-sided filter. The result of this fact is that it is most likely unnecessary to pursue the compensation technique any further.
- The remaining performance loss after adaptive suppression using either the compensated predictive filter or the two-sided filter is largely due to the loss of signal energy in the suppression process. Very little loss is due to residual jammer, i.e. jammer that is not suppressed by the adaptive filtering.
- As the order of the two-sided filter increases, the performance approaches that for BPSK in AWGN alone for strong jammers, assuming that the loss in signal power incurred in the jammer suppression process is taken into account. This result indicates that distortion of the code portion of the signal during the jammer suppression process is not a serious problem.
- The presence of multipath propagation has a serious detrimental effect on the performance of receivers equipped with the adaptive suppressors. The multipath introduces correlation into the DSSS portion of the signal, enabling the adaptive suppressors to cancel some of this desired signal.

7.1 Future Work

There are several areas which require further study:

- Develop an approach which allows the two-sided adaptive suppressor to suppress the interference without suppressing the DSSS signal in the presence of multipath. Since multipath is a common channel property in radio communications, it is essential that an interference suppression technique be able to function properly in its presence.
- Develop a structure which merges the multipath energy combining property of the RAKE receiver with the interference suppression capability of the two-sided adaptive filter. In the best case, it is desirable not only to be able to tolerate multipath but to be able to *take advantage* of the time diversity produced by the multipath to improve performance.

Bibliography

- [1] L.B. Milstein. Interference rejection techniques in spread spectrum communications. *Proc. IEEE*, 76, no. 6:657–671, June 1988.
- [2] F. M. Hsu and A.A. Giordano. Digital whitening techniques for improving spread spectrum communications performance in the presence of narrowband jamming and interference. *IEEE Trans. Commun.*, COM-26:209–216, Feb. 1978.
- [3] L-M Li and L.B. Milstein. Rejection of narrow-band interference in pn spread-spectrum systems using transversal filters. *IEEE Trans. Commun.*, COM-30:925–928, May 1982.
- [4] J.W. Ketchum and J. G. Proakis. Adaptive algorithms for estimating and suppressing narrow-band interference in pn spread-spectrum systems. *IEEE Trans. Commun.*, COM-30:913–924, May 1982.
- [5] R. A. Iltis and L. B. Milstein. Performance analysis of narrow-band interference rejection techniques in DS spread-spectrum systems. *IEEE Trans. Commun.*, COM-32:1169–1177, Nov. 1984.
- [6] G.R. Cooper. Tone jammer cancellation in a tapped-delay line correlator. In *IEEE Military Communications Conf.*, pages 469–473, 1984.
- [7] G.J. Saulnier, P.K. Das, and L.B. Milstein. An adaptive digital suppression filter for direct sequence spread spectrum communications. *IEEE J. Selected Areas Commun.*, SAC-3, no. 5:676–686, Sept. 1985.
- [8] C. N. Pateros and G. J. Saulnier. An adaptive correlator receiver for direct sequence spread spectrum communication. *IEEE Transactions on Communications*, 44(10), November 1996.
- [9] R. A. Iltis and L. B. Milstein. An approximate statistical analysis of the Widrow LMS algorithm with application to narrow-band interference rejection. *IEEE Trans. Commun.*, COM-33:121–130, Feb. 1985.
- [10] R. Price and P.E. Green, Jr. A communication technique for multipath channels. *Proc. IRE*, 46:555–570, Mar. 1958.

[11] J. G. Proakis. *Digital Communications*. McGraw-Hill, 1989.

***MISSION
OF
AFRL/INFORMATION DIRECTORATE (IF)***

The advancement and application of information systems science and technology for aerospace command and control and its transition to air, space, and ground systems to meet customer needs in the areas of Global Awareness, Dynamic Planning and Execution, and Global Information Exchange is the focus of this AFRL organization. The directorate's areas of investigation include a broad spectrum of information and fusion, communication, collaborative environment and modeling and simulation, defensive information warfare, and intelligent information systems technologies.